Astronomy & Astrophysics manuscript no. ms
January 22, 2014
© ESO 2014

arXiv:1401.5388v1 [astro-ph.SR] 21 Jan 2014

Rayleigh-Taylor instability in partially ionized compressible plasmas; one fluid approach

A. J. Díaz[1,2], E. Khomenko[1,2] & M. Collados[1,2]

[1] Instituto de Astrofísica de Canarias, 38205, C/ Vía Láctea, s/n, La Laguna, Tenerife, Spain
[2] Departamento de Astrofísica, Universidad de La Laguna, 38205, La Laguna, Tenerife, Spain
e-mail: tdiaz@iac.es; khomenko@iac.es; mcv@iac.es

Received / Accepted

ABSTRACT

Aims. We study the modification of the classical criterion for the linear onset and growth rate of the Rayleigh-Taylor instability (RTI) in a partially ionized (PI) plasma in the one-fluid description, considering a generalized induction equation.
Methods. The governing linear equations and appropriate boundary conditions, including gravitational terms, are derived and applied to the case of the RTI in a single interface between two partially ionized plasmas. The boundary conditions lead to an equation for the frequencies in which some of them have positive complex parts, marking the appearance of the RTI. We study the ambipolar term alone first, extending the result to the full induction equation later.
Results. The configuration is always unstable because of the presence of a neutral species. In the classical stability regime the growth rate is small, since the collisions prevent the neutral fluid to fully develop the RTI. For parameters in the classical instability regime the growth rate is lowered, but for the considered theoretical values of the collision frequencies and diffusion coefficients for solar prominences the differences with the compressible MHD case are small.
Conclusions. PI modifies some aspects of the linear RTI instability, since it takes into account that neutrals do not feel the stabilizing effect of the magnetic field. For the set of parameters representative for solar prominences, our model gives the resulting timescale comparable with observed lifetimes of RTI plumes.

Key words. Instabilities, Sun: oscillations, Sun: corona, Sun: filaments, prominences

1. Introduction

One of the well-known fluid instabilities that has been applied widely in many different astrophysical contexts is the Rayleigh-Taylor instability (RTI for short), which appears when a lighter fluid supports or accelerates a heavier one. We can cite as examples the RTI in planetary nebulas (Bucciantini et al. 2004), supernova explosions (Fryxell et al. 1991), acretion disks (Wang & Nepveu 1983), relativistic jets (Matsumoto & Masada 2013), the evolution of the inner layers of red giants (Eggleton et al. 2006), formation of hydrogen clouds in the local bubble (Breitschwerdt et al. 2000) or the solar atmospheric flux tubes (Parker 1979) or prominences (Isobe et al. 2005), for citing some topics among the vast literature regarding this instability in astrophysical plasmas.

The starting point of these studies is the classical hydrodynamic instability, with the addition of a magnetic field. To study the Rayleigh-Taylor instability in Magnetohydrodynamics (MHD), it is better to use the divergence-free velocity condition (which is the type of movement more likely to produce instabilities, since the energy is not wasted in compressing the plasma). Hence, the dispersion relation for the two fluids with densities ρ_1 and ρ_2 laying one below the other with a magnetic field parallel to the contact surface is (Chandrasekhar 1961; Priest 1982),

$$\omega^2 = -gk\frac{\rho_2 - \rho_1}{\rho_1 + \rho_2} + \frac{2B_0^2 k_x^2}{\mu(\rho_1 + \rho_2)}, \quad (1)$$

where B_0 is the magnetic field strength and k is the modulus of the wavenumber, k_x is the component of the wavenumber along the magnetic field direction and k_y the component across the field, g is the acceleration of gravity, and μ is the magnetic permittivity. The hydromagnetic case is recovered if no magnetic field is considered, which means that the configuration is unstable if $\rho_2 > \rho_1$. The magnetic field stabilizes perturbations down to a critical value of k_x along its direction, but the field cannot stabilize perturbations across the field ($k_x = 0$), no matter how strong it might be.

Other effects, such as compressibility, viscosity, tension forces, relativistic corrections, magnetic fields perpendicular to the surface or other types of stratification and forces, may introduce corrections to the classical stability criterion and linear growth rate of the RTI. The leading one is normally the compressibility, which must be taken into account in most of the applications. There have been many studies of the effect of compressibility in the magnetic RTI (see for example Vandervoort 1961; Shivamoggi 1982; Bernstein & Book 1983; Ribeyre et al. 2004; Livescu 2004; Shivamoggi 2008; Liberatore & Bouquet 2008, and references therein). These studies show that the compressibility has mainly a stabilizing influence by lowering the linear growth rates, although the stability threshold that appears in Eq. 1 is not modified. On the other hand, even considering only this extra effect complicates greatly the solution, so simple relations such as Eq. 1 are no longer obtained.

Prominences are a very likely candidate to display the RTI in the solar atmosphere, since they are composed of cool and dense plasma surrounded by much lighter coronal plasma (see the reviews Labrosse et al. 2010; Mackay et al. 2010). The magnetic field plays a key role in the structure and dynamics of prominences, and hence the RTI must be studied in the context of the MHD theory. Using computational techniques allow us to solve directly the MHD partial differential equations and study the non-linear regime of the RTI. These numerical studies of RTI (see for example Jun et al. 1995; Arber et al. 2007; Stone & Gardiner 2007) agree with the results of the linear theory and show some new interesting features, such as the enhancement of the growth of bubbles and fingers in the non-linear regime across the field, since it prevents secondary Kelvin-Helmholtz instabilities and mixing between the fluids. This non-linear phase agrees qualitatively with the observations of turbulent plumes and bubbles in prominences (Isobe et al. 2005; Berger et al. 2008; Heinzel et al. 2008; Ryutova et al. 2010; Berger et al. 2010, 2011) and has even been used to infer plasma properties from observational features (Hillier et al. 2012b). The presence of the RTI has also been confirmed numerically in more general prominence models with 3D geometry (Isobe et al. 2006; Hillier et al. 2011, 2012a,c).

Prominences have also another feature that can be relevant for the RTI because of their physical properties, namely partial ionization. Since prominences are relatively cool and dense objects, their plasma is expected to be partially ionized (Patsourakos & Vial 2002; Gilbert et al. 2007; Labrosse et al. 2010; Zaqarashvili et al. 2011b). The ionization degree of the prominence plasma has not been directly measured with accuracy, but with the typical physical properties of the plasma the plasma is neither in a completely ionized state or is a neutral gas. This partially ionized prominence plasma can no longer be described with 1-fluid ideal MHD. Chhajlani & Vaghela (1989) studied the magnetic RTI in a two fluid model without considering the full dynamics of the neutral fluid (which was only subject to collisions) and concluded that the stability threshold is not changed, but the growth rate is lowered. A two-fluid description with a neutral and an ion-electron fluids coupled only by ion-neutral collision (without electron collisions and diffusive terms in the induction equation) was considered in Soler et al. (2012b) for the Kelvin-Helmholtz instability due to shear flow at an interface between two partially ionized plasmas and in Díaz et al. (2012) for the RTI in a similar setup. The conclusion in Díaz et al. (2012) was that the instability threshold of the RTI is modified, so the configuration with heavier fluid on the top of lighter fluid is always unstable, but that the linear growth rate is substantially reduced depending on the parameters. This approach has also been used by Shadmehri et al. (2013) in the context of the RTI in the borders of the local bubble, where partial ionization also plays a relevant role.

Our main objective in this paper is to study the stability threshold and the linear growth rate of the RTI in a plasma described in a single-fluid model, taking into account the partial ionization effects in the form of a generalized induction equation and considering all the types of collisions and forces present and the diffusive terms in the induction equation. We develop a rather general formulation, with an aim of its global applicability different astrophysical situations. After this general formulation has been set, we particularize to the case of solar prominence and consider the importance of different terms in the induction equations (many of them have been neglected in the previous works) on the development of the RTI in this environment. We compare our results with those from the simple two-fluid approach in Díaz et al. (2012) and try to understand the linear phase of the RTI in a partially ionized plasma to use it as a comparison with more complicated computational models with geometrically complex geometry and the non-linear stages.

2. Multifluid equations for partially ionized plasma

2.1. Fluid equations for each species

The general transport equations for a multi-component plasma can be derived from the Boltzmann kinetic equation, taking into acount general properties of he collisions terms (Braginskii 1965; Bittencourt 1986; Balescu 1988). The most common form of the MHD theory can only be applied to totally ionized plasma, where the different species are completely coupled dinamically and thermally by collisions, so partial ionization cannot be described. The first extension from MHD in the presence of neutrals for strong collisional coupling is to consider only the modifications due to collisions in the generalized Ohm's law and energy transport (Braginskii 1965; Khodachenko et al. 2004; Forteza et al. 2007), assuming a strong thermal coupling and neglecting the transport coefficients. Another way of including partial ionization effects is to use a multi-fluid treatment, in which ions and electrons are considered together as an ion-electron fluid (due to their strong electromagnetic coupling), and neutrals are considered separately with as many neutral species as one wishes to include (see, e.g., Zaqarashvili et al. 2011b,a; Soler et al. 2012a). The two-fluid approach (a hydrogen plasma only considered) was used in Díaz et al. (2012) for studing the RTI, with the additional neglection of other diffusive terms in the induction equation. Here we take the single fluid approach by combining the equations for each species in a single fluid equation, and obtaining a generalized form of the MHD equations valid for PI plasmas.

We proceed with the derivation of the generalized one fluid equations starting from the macroscopic equations for each species. In the following expressions the subscripts i, n and e stand for ions, neutrals and electrons, respectively. The momentum equation for each species is

$$\begin{aligned}
\rho_e \left(\frac{\partial \mathbf{v}_e}{\partial t} + \mathbf{v}_e \cdot \nabla \mathbf{v}_e \right) &= -\nabla p_e - e n_e \left(\mathbf{E} + \mathbf{v}_e \times \mathbf{B} \right) \\
&+ \rho_e \mathbf{g} + \mathbf{R}_e, \\
\rho_i \left(\frac{\partial \mathbf{v}_i}{\partial t} + \mathbf{v}_i \cdot \nabla \mathbf{v}_i \right) &= -\nabla p_i + e n_i \left(\mathbf{E} + \mathbf{v}_i \times \mathbf{B} \right) \\
&+ \rho_i \mathbf{g} + \mathbf{R}_i, \\
\rho_n \left(\frac{\partial \mathbf{v}_n}{\partial t} + \mathbf{v}_n \cdot \nabla \mathbf{v}_n \right) &= -\nabla p_n + \rho_n \mathbf{g} + \mathbf{R}_n, \qquad (2)
\end{aligned}$$

where $\mathbf{v}_i$, $\mathbf{v}_e$ and $\mathbf{v}_n$ are the velocity of the ion, electron and neutral fluid, respectively, p_i, p_e and p_n are the pressure of the ion, electron and the neutral fluid, respectively, ρ_i, ρ_e and ρ_n are the ion, electron and neutron densities, respectively, and R_i, R_e and R_n are the momentum transfer terms due to collisions for ions, electrons and neutrals, respectively. We also define the total density $\rho = \rho_n + \rho_i$, the

neutral fraction $\xi_n = \rho_n/\rho$ and the ion fraction $\xi_i = \rho_i/\rho$, with $\xi_n + \xi_i = 1$. Hence, the parameter ξ_n indicates the ionization degree, from $\xi_n = 0$ for a fully ionized plasma to $\xi_n = 1$ for a neutral gas. We have assumed the non diagonal terms of the pressure tensors to be negligible and the diagonal terms to be equal, so the pressure tensor becomes isotropic and can be represented by the scalar pressure. The elastic collision term of each species is approximated as (Braginskii 1965; Bittencourt 1986)

$$\mathbf{R}_\alpha = -\rho_\alpha \sum_\beta \nu_{\alpha\beta}(\mathbf{v}_\alpha - \mathbf{v}_\beta) \tag{3}$$

where $\nu_{\alpha\beta}$ is the collisional frequency of species α with particles of species β. So, for our three species they become:

$$\begin{aligned}
\mathbf{R}_e &= -\rho_e(\nu_{ei}(\mathbf{v}_e - \mathbf{v}_i) + \nu_{en}(\mathbf{v}_e - \mathbf{v}_n)) \\
&= \rho_e \frac{1}{n_i e}\mathbf{J}(\nu_{ei} + \nu_{en}) - \rho_e \nu_{en}\mathbf{w} \\
\mathbf{R}_i &= -\rho_i(\nu_{ie}(\mathbf{v}_i - \mathbf{v}_e) + \nu_{in}(\mathbf{v}_i - \mathbf{v}_n)) \\
&= -\rho_i \frac{1}{n_i e}\nu_{ie}\mathbf{J} - \rho_i \nu_{in}\mathbf{w} \\
\mathbf{R}_n &= -\rho_n(\nu_{ni}(\mathbf{v}_n - \mathbf{v}_i) + \nu_{ne}(\mathbf{v}_n - \mathbf{v}_e)) \\
&= -\rho_n \frac{1}{n_i e}\nu_{ne}\mathbf{J} - \rho_n(\nu_{ni} + \nu_{ne})\mathbf{w},
\end{aligned} \tag{4}$$

with $\mathbf{w} = \mathbf{v}_i - \mathbf{v}_n$ the diffusion velocity of ions with respect to neutrals and $\mathbf{J} = en_e(\mathbf{v}_i - \mathbf{v}_e)$ the total current density. This form of the friction momentum transfer does not alter the one-fluid equations of mass conservation and momentum conservation from their MHD counterparts when written in terms of the overall velocity of the plasma, $\mathbf{v} = \sum_{\alpha=i,e,i}(\rho_\alpha \mathbf{v}_\alpha)/\rho \approx \xi_i \mathbf{v}_i + \xi_n \mathbf{v}_n$. However, the energy equation has to take into account the currents arising from these non-MHD terms, and an additional equation for the evolution of the magnetic field is also required to close the system, namely a generalized induction equation.

2.2. Equation for the diffusion velocity

To obtain the momentum equation for the diffusion velocity $\mathbf{w}$ we proceed as follows. The momentum equation for electrons and ions are added up, neglecting the electron inertial terms because of the small electron mass compared to the other species. We are not neglecting the electron gravity compared with the ion gravity yet ($\rho_e\mathbf{g}$ compared to $\rho_i\mathbf{g}$),

$$\begin{aligned}
\rho_i\left(\frac{\partial \mathbf{v}_i}{\partial t} + \mathbf{v}_i \cdot \nabla \mathbf{v}_i\right) &= \mathbf{J}\times\mathbf{B} + (\rho_i + \rho_e)\mathbf{g} - \nabla(p_i + p_e) \\
&\quad - \alpha_n \mathbf{w} + \rho_n \nu_{ne}\frac{1}{n_i e}\mathbf{J} \\
\rho_n\left(\frac{\partial \mathbf{v}_n}{\partial t} + \mathbf{v}_n \cdot \nabla \mathbf{v}_n\right) &= \rho_n \mathbf{g} - \nabla p_n + \alpha_n \mathbf{w} \\
&\quad - \rho_n \nu_{ne}\frac{1}{n_i e}\mathbf{J},
\end{aligned} \tag{5}$$

with the definition for the coefficient of friction between the plasma and the neutral gas

$$\alpha_n = \rho_n(\nu_{ni} + \nu_{ne}) = \rho_i \nu_{in} + \rho_e \nu_{en}. \tag{6}$$

Now we add the upper equation multiplied by ξ_n and lower equation, multiplied by $-\xi_i$. The result is:

$$\begin{aligned}
\xi_i\xi_n\rho\left(\frac{D_i\mathbf{v}_i}{Dt} - \frac{D_n\mathbf{v}_n}{Dt}\right) &= \xi_n[\mathbf{J}\times\mathbf{B}] - \mathbf{G} - \alpha_n\mathbf{w} \\
&\quad + \rho_n\nu_{ne}\frac{1}{n_i e}\mathbf{J} + \xi_n\rho_e\mathbf{g},
\end{aligned} \tag{7}$$

where

$$\frac{D_\alpha}{Dt} = \frac{\partial}{\partial_t} + v_\alpha \cdot \nabla. \tag{8}$$

We have taken into account that $\xi_i + \xi_n = 1$, thus the gravity terms for ions and neutrals cancel out and the electron term might become relevant. This gravitional term is in fact similar to those of the electron inertia that have been already neglected, but we keep it here to check its magnitude, specially since the RTI is driven by gravity so it is important to assure its effect as much as possible. Regarding the pressure gradients, we have introduced the new PI pressure terms following Braginskii (1965) as

$$\mathbf{G} = \xi_n \nabla(p_i + p_e) - \xi_i \nabla p_n. \tag{9}$$

We still have the ion and neutral inertia terms in Eq. (7). These are neglected on the basis of the following argument. We can express the total derivative in terms of the diffusion velocity

$$\begin{aligned}
\left(\frac{D_i\mathbf{v}_i}{Dt} - \frac{D_n\mathbf{v}_n}{Dt}\right) &= \frac{\partial \mathbf{w}}{\partial t} + (\xi_n - \xi_i)\mathbf{w}\cdot\nabla\mathbf{w} + \\
&\quad \mathbf{w}\cdot\nabla\mathbf{v} + \mathbf{v}\cdot\nabla\mathbf{w}. \approx \frac{\partial \mathbf{w}}{\partial t}.
\end{aligned} \tag{10}$$

In a linear regime all the advection terms in this equation are second order effects, and the remaining time derivative of $\mathbf{w}$ can be neglected when compared with the friction terms, which are of the order of $\mathbf{w}/\tau_{\rm col}$, with $\tau_{\rm col} \sim 1/\nu_{\alpha\beta}$ being the characteristic timescale related to collisions.

Taking all the aforementioned simplifications into account, we obtain an expression for the diffusion velocity between ions and neutrals,

$$\mathbf{w} = \frac{\xi_n}{\alpha_n}\mathbf{J}\times\mathbf{B} - \frac{\mathbf{G}}{\alpha_n} + \rho_n\nu_{ne}\frac{1}{n_i e\alpha_n}\mathbf{J} + \frac{\xi_n\rho_e}{\alpha_n}\mathbf{g}. \tag{11}$$

From this expression we can see that the ion and neutral fluids do not follow each other exactly, which raises additional dissipative effects. On the other hand, by neglecting the inertial terms we have obtained an explicit expression for the diffision velocity in terms of other variables, assuming that collissions lead to the terminal values of $\mathbf{w}$ given by Eq. (11) much faster than the evolution of the remaining variables. Thus, the velocities of the ion and neutral species do not longer appear in the equations and the diffusion velocity $\mathbf{w}$ can be computed from the single-fluid variables.

2.3. Induction Equation

To proceed further we need a generalized Ohm's law and an induction equation to obtain an equation for the magnetic field evolution. These are obtained from the momentum equation for electrons in Eq. 2, neglecting again their inertial terms. We obtain after some algebra

$$\begin{aligned}
\mathbf{E} + \mathbf{v}\times\mathbf{B} &= -\xi_n\,\mathbf{w}\times\mathbf{B} + \frac{1}{n_i e}\mathbf{J}\times\mathbf{B} \\
&\quad - \frac{\nabla p_e}{e n_e} + \alpha_e\frac{1}{n_i^2 e^2}\mathbf{J} - \frac{\rho_e\nu_{en}\mathbf{w}}{e n_e} + \frac{\rho_e}{n_e e}\mathbf{g},
\end{aligned} \tag{12}$$

with the definition $\alpha_e = \rho_e(\nu_{ei} + \nu_{en})$. We then substitute the expression for the diffusion velocity in Eq. (11) and insert the result in Faraday's law, obtaining

$$\begin{aligned}\frac{\partial \mathbf{B}}{\partial t} &= \nabla \times \left[(\mathbf{v}\times\mathbf{B}) - \frac{\mathbf{J}}{\sigma} - \left(\frac{1-2\varepsilon\xi_n}{en_e}\mathbf{J}\times\mathbf{B}\right)\right. \\ &+ \left(\frac{\xi_n^2}{\alpha_n}(\mathbf{J}\times\mathbf{B})\times\mathbf{B}\right) - \left(\frac{\varepsilon\mathbf{G}-\nabla p_e}{en_e}\right) \\ &- \left(\frac{\xi_n}{\alpha_n}\mathbf{G}\times\mathbf{B}\right) - \left(\frac{\rho_e}{en_e}(1+\xi_n\varepsilon)\mathbf{g}\right. \\ &+ \left.\left.\frac{\xi_n^2\rho_e}{\alpha_n}\mathbf{g}\times\mathbf{B}\right)\right] \end{aligned} \quad (13)$$

with the definitions of $\varepsilon = \rho_e\nu_{en}/\alpha_n$ (which is a small parameter) and the Ohmic conductivity $\sigma = (en_e)^2/(\alpha_e - \varepsilon^2\alpha_n)$. In this equation, the terms on the right hand side are: ideal MHD induction term, Ohmic term, Hall term, ambipolar term, generalized battery term (which includes a part already present in plasmas and a part depending on partial ionization by means of $\mathbf{G}$), a $\mathbf{G}\times\mathbf{B}$ term of perpendicular currents caused by these pressure gradients (similar to the Hall term with currents) and gravity terms (again with a similar $\mathbf{g}\times\mathbf{B}$ part also included). We can define the coefficients in the different terms as

$$\begin{aligned}\eta &= \frac{1}{\sigma\mu} = \frac{\alpha_e - (\rho_e\nu_{en})^2/\alpha_n}{(en_e)^2\mu}, \\ \eta_{\rm H} &= \frac{1-2\varepsilon\xi_n}{en_e\mu}B_0, \\ \eta_{\rm A} &= \frac{\xi_n^2}{\alpha_n\mu}B_0^2, \\ \chi_{\rm p} &= \frac{\xi_n}{\alpha_n}, \\ \chi_{\rm g} &= \frac{\xi_n^2\rho_e}{\alpha_n}, \end{aligned} \quad (14)$$

with η, $\eta_{\rm H}$, $\eta_{\rm A}$, $\chi_{\rm p}$ and $\chi_{\rm g}$ being the ohmic diffusivity, Hall diffusivity, ambipolar diffusivity and coefficients related to the battery and gravity terms, respectively. Assuming that the acceleration of gravity is uniform, the curl of the prelast term in Eq. 13 vanishes, and the induction equation is finally written as

$$\begin{aligned}\frac{\partial \mathbf{B}}{\partial t} &= \nabla \times \left[(\mathbf{v}\times\mathbf{B}) - \eta\nabla\times\mathbf{B} - \eta_{\rm H}(\nabla\times\mathbf{B})\times\mathbf{B}/B_0\right. \\ &+ \eta_{\rm A}\{(\nabla\times\mathbf{B})\times\mathbf{B}\}\times\mathbf{B}/B_0^2 - (\varepsilon\mathbf{G}-\nabla p_e)/(en_e) \\ &- \left.\chi_{\rm p}\mathbf{G}\times\mathbf{B} - \chi_{\rm g}\mathbf{g}\times\mathbf{B}\right], \end{aligned} \quad (15)$$

in which we used Ampere's law (neglecting Maxwell's displacement current) to eliminate the current density in terms of the magnetic field, $\mathbf{J} = \nabla\times\mathbf{B}/\mu$. Eq. 15 is a very general form of the induction equation in the one fluid description of partial ionized plasmas, and it is in fact a generalization of the well-known generalized induction equation in classical textbooks (see for example Braginskii 1965) with all the pressure gradient and gravity terms included and the expressions of the diffusion coefficients.

The formulation of the induction equation in Eq. (15) allows for the very general analysis, that can be useful in a broad context of astrophysical plasmas. Some of the terms are a priory expected to be smaller than others (as those related to the electron mass), but others can not be ruled out just from general considerations. Below we will discuss their importance for the case of the parameters appropriate for solar prominences. We next describe the plasma and magnetic field configuration used to study the RTI in this environment in Sect. 3 and then explore in Sect. 4 the effect of the leading term under these conditions, namely the ambipolar diffusion $\eta_{\rm A}\{(\nabla\times\mathbf{B})\times\mathbf{B}\}\times\mathbf{B}/B_0^2$. Then, we consider the full induction equation in Sect. 5 to test the magnitude of the remaining terms and finish discussing the results and drawing our conclusions.

3. Reference configuration

Since we are aiming to obtain some extensions to the well known formula in Equation (1) we restrict the analysis to the simple configuration of a contact surface following the classical analysis in (Chandrasekhar 1961; Drazin & Reid 1981; Priest 1982), amenable to analytical solutions. We use this configuration to study the RTI in prominence threads, specially for choosing the values of the equilibrium and perturbation parameters, but the method developed in this paper is general and can be applied to other astrophysical situations which involve the RTI in PI plasmas.

The reference configuration consists of two regions filled with uniform plasmas composed of ions, electrons and neutrals separated by a contact surface at $z = 0$. We use Cartesian coordinates and denote the quantities in the plasma below the discontinuity ($z < 0$) with a subscript 1 and those in the plasma above the discontinuity ($z > 0$) with a subscript 2. The magnetic field permeating the plasma is uniform and tangent to the discontinuity, so $\mathbf{B} = B_0\hat{x}$, while gravity is perpendicular to it, so $\mathbf{g} = -g\hat{z}$. The whole configuration is invariant in the x and y-directions.

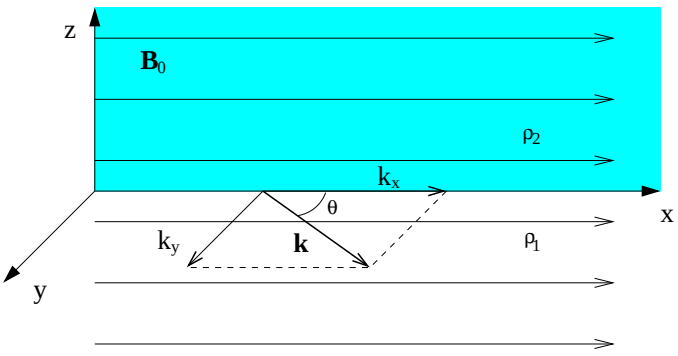

Fig. 1. Sketch of the equilibrium configuration used in the analysis of this work. The equilibrium state is a contact surface between two regions filled uniformly with plasma having different properties, with the lower quantities labelled as "1" and the upper ones as "2". The magnetic field is uniform and directed along the x-axis, while the whole configuration is invariant in the x and y-directions.

In absence of hydrostatic pressure gradients or flows, the plasma described in the previous paragraph is not in equilibrium, since nothing counteracts the gravity force. We are not interested in the overall equilibrium, only in the local region where the instability is triggered. More precisely, the equilibrium pressure gradient ∇p_0 is related to the gravitational scale height, while the perturbed quantities vary

on a much shorter spatial scale. Hence, we assume that all the plasma magnitudes (namely the density, the pressure and the ionization degree) are constant in each zone. Pressure balance along the discontinuity demands that the total pressure for each species must be equal in each side, and since the magnetic field is assumed to be uniform this means the gas pressures are equal in each side ($p_1 = p_2$). On the other hand, the temperature, density and ionization degree on each region are parameters of our model. Since we are interested in studing the RTI we assume that $\rho_2 > \rho_1$. No ionization-recombination processes are included, so the ionization degree in each region remains constant. Note also that the plasma beta $\beta = c_{\rm s2}^2/c_{\rm A2}^2 = c_{\rm s1}^2/c_{\rm A1}^2 = \gamma\mu p_2/B_0^2$ is then constant all over the domain.

Another important simplification in this particular configuration is that we can neglect the variations of the coefficients in Eq. (14) during the evolution of the instability. The equilibrium field satisfies $\nabla \times \mathbf{B}_0 = 0$, so there are no currents in the reference state and the only contribution of the diffusive terms to the first-order induction equation are those with the coefficients calculated in the reference configuration.

Finally, using this reference configuration the classical instability criterion (Eq. 1) can be written in the following form

$$\omega^2 = 2\left(\overline{c}_{\rm A}{}^2 \cos^2\theta - c_{\rm crit}^2\right) k^2, \tag{16}$$

with θ being the angle between the equilibrium magnetic field and the wavevector $\mathbf{k}$ and k the wavevector modulus (wavenumber). We define the critical speed as

$$c_{\rm crit} = \left(\frac{g}{2k}\,\frac{\rho_2-\rho_1}{\rho_2+\rho_1}\right)^{1/2}, \tag{17}$$

and the reduced square Alfvén speed as

$$\overline{c}_{\rm A} = \left(\frac{B_0}{\mu_0(\rho_1+\rho_2)}\right)^{1/2}, \tag{18}$$

with usual definition for the squared Alfvén speed $c_{\rm A}^2 = B_0^2/(\mu\rho_0)$, so $\overline{c}_{\rm A}{}^{-2} = (c_{\rm A1})^{-2} + (c_{\rm A2})^{-2}$ It is convenient then to use $\overline{c}_{\rm A}$ as a parameter, and notice that in the case of a prominence with $\rho_2 \gg \rho_1$ we have $\overline{c}_{\rm A} \approx c_{\rm A2}$, so this averaged Alfvén speed is approximately the Alfvén speed in the prominence.

4. MHD plus ambipolar diffusion

It is clear that dealing with the all the terms in Eq. 15 is very difficult. Hence, we concentrate first in the modifications introduced in the ideal MHD theory by the ambipolar term, which has proved to be relevant in solar atmospheric situations (see for example Khodachenko et al. 2004; Arber et al. 2007; Khomenko & Collados 2012, and references therein). We neglect in this section all the magnetic diffusion terms except the ambipolar one, obtaining a simple form of the induction equation,

$$\frac{\partial \mathbf{B}}{\partial t} = \nabla \times \left(\mathbf{v}\times\mathbf{B} + \eta_{\rm A}\left\{(\nabla\times\mathbf{B})\times\mathbf{B}\right\}\times\mathbf{B}/B_0^2\right). \tag{19}$$

The mass and momentum conservation equations are not modified by the presence of ambipolar diffusion. In addition, we assume an adiabatic energy equation plus the contribution from the ambipolar diffusion term (neglecting transport terms such as conduction, radiation of other heating sources). Hence, after deriving the energy term corresponding to the ambipolar diffusion, our system of basic equations is

$$\begin{aligned}
\frac{\partial \rho}{\partial t} &= -\nabla\cdot(\rho\mathbf{v}),\\
\rho\frac{\partial \mathbf{v}}{\partial t} &= -\rho\mathbf{v}\cdot\nabla\mathbf{v} - \nabla p + \frac{1}{\mu}(\nabla\times\mathbf{B})\times\mathbf{B} + \rho\mathbf{g},\\
\frac{\partial \mathbf{B}}{\partial t} &= \nabla\times\left(\mathbf{v}\times\mathbf{B} + \eta_{\rm A}\left\{(\nabla\times\mathbf{B})\times\mathbf{B}\right\}\times\mathbf{B}/B_0^2\right),\\
\frac{\partial p}{\partial t} &= -\mathbf{v}\cdot\nabla p - \gamma p\nabla\cdot\mathbf{v}\\
&\quad +(\gamma-1)\frac{\eta_{\rm A}}{\mu B_0^2}(\nabla\times\mathbf{B})\times[\{(\nabla\times\mathbf{B})\times\mathbf{B}\}\times\mathbf{B}],
\end{aligned} \tag{20}$$

where γ is the adiabatic index and $p = p_i + p_e + p_n$ the total scalar pressure of the fluid.

4.1. Linearized equations

Next, we study linear perturbations from the uniform state. To obtain a general formulation, we label the reference quantities with the subscript 0 and the linear perturbations without subscript ($\mathbf{B} = B_0\mathbf{x} + \mathbf{b}$). The subscript 0 can be replaced with 1 of 2 when one of the regions in which the physical domain is considered, but otherwise, the deduction is valid for any uniform configuration.

Since no equilibrium flow is present ($\mathbf{v}_0 = 0$), all the advection terms are second order effects. No currents are present in the reference state, so the term in the energy equation coming from the ambipolar diffusion is also a second order effect and can be neglected in the linealized problem. Hence, we are left with a considerably simpler system of differential equations, namely

$$\begin{aligned}
\frac{\partial \rho}{\partial t} &= -\rho_0\nabla\cdot\mathbf{v},\\
\rho_0\frac{\partial \mathbf{v}}{\partial t} &= -\nabla p + \frac{1}{\mu}(\nabla\times\mathbf{b})\times\mathbf{B}_0 + \rho\mathbf{g},\\
\frac{\partial \mathbf{b}}{\partial t} &= \nabla\times\left(\mathbf{v}\times\mathbf{B}_0 + \frac{\eta_{\rm A}}{B_0^2}\left\{(\nabla\times\mathbf{b})\times\mathbf{B}_0\right\}\times\mathbf{B}_0\right),\\
\frac{\partial p}{\partial t} &= -\gamma p_0\nabla\cdot\mathbf{v}.
\end{aligned} \tag{21}$$

This system of equations can be reduced to only two by taking the time derivative of the momentum equation and substituting the expressions for the density and pressure from the continuity and energy equations, respectively, obtaining a system of two partial differential equation for the perturbations in velocity and magnetic field, namely

$$\begin{aligned}
\frac{\partial^2 \mathbf{v}}{\partial t^2} &= c_{\rm A}^2\left(\nabla\times\frac{\partial \mathbf{b}}{\partial t}\right)\times\mathbf{B}_0 - (\nabla\cdot\mathbf{v})\,\mathbf{g} + c_{\rm s}^2\nabla(\nabla\cdot\mathbf{v}),\\
\frac{\partial \mathbf{b}}{\partial t} &= \nabla\times\left(\mathbf{v}\times\mathbf{B}_0 + \frac{\eta_{\rm A}}{B_0^2}\left\{(\nabla\times\mathbf{b})\times\mathbf{B}_0\right\}\times\mathbf{B}_0\right),
\end{aligned} \tag{22}$$

We have defined the squared sound speed as $c_{\rm s}^2 = \gamma p_0/\rho_0$. The equilibrium properties of the medium relevant for the RTI are included in the sound and Alfvén speeds, together with the ambipolar diffusivity coefficient. In our problem is not possible to derive a single equation by eliminating the

Lorentz force term in the motion equation by using the induction equation as is routinely done in ideal MHD (see for example Roberts 1981; Priest 1982; Goedbloed & Poedts 2004).

We are left with only one parameter depending on the ionization fraction, the ambipolar diffusivity $\eta_{\rm A}$ (Eq. (14), which is calculated in the equilibrium state and depends on the ionization degree ξ_n and the neutral friction coefficient (Eq. 6),

$$\alpha_n = \rho_0(1-\xi_n)(\nu_{in} + \nu_{en} m_e/m_i). \tag{23}$$

We can neglect the term with the ratio of the electron and ion mass and use the expression for the ion-neutral collision frequency in a plasma (see, e.g., Braginskii 1965; Soler et al. 2009),

$$\nu_{in} = \frac{\rho_n}{m_{\rm n}}\sqrt{\frac{16 k_{\rm B} T}{\pi m_{\rm n}}}\,\sigma_{\rm in}, \tag{24}$$

where T is the temperature, $m_{\rm n}$ the neutron mass, $k_{\rm B}$ is the Boltzmann constant and $\sigma_{\rm in} \approx 5\times10^{-19}$ m^2 is the collisional cross section for proton-hydrogen collisions (assuming a hydrogen plasma). Notice that this collision frequency is a theoretical value for hard-sphere collisions between protons and H molecules, while there are hints that actual values can differ from this simple calculation (Mitchner & Kruger 1973; Vranjes & Krstic 2013). A strong thermal coupling is assumed, so the temperature of the different species is the same. Hence, $k_{\rm B}T/m_n = p_n/\rho_n = (2-\xi_n)^{-1} c_{\rm s}^2/\gamma$ and the expression for the friction coefficient is

$$\alpha_n = \frac{4\sigma_{\rm in}}{m_{\rm n}\,(\pi\gamma)^{1/2}}\,\rho_0^2 c_{\rm s}\frac{\xi_n(1-\xi_n)}{(2-\xi_n)^{1/2}}, \tag{25}$$

Finally, we obtain from Eq. (14) an equation for $\eta_{\rm A}$, in therms of the equilibrium parameters in each region.

$$\eta_{\rm A} = \frac{m_{\rm n}\,(\pi\gamma)^{1/2}}{4\sigma_{\rm in}}\,\frac{\xi_n(2-\xi_n)^{1/2}}{1-\xi_n}\,\frac{c_{\rm A}^2}{\rho_0 c_{\rm s}}. \tag{26}$$

This expression depends on the medium density. We use $\rho_0 = 10^{10}$ kg m^{-3} for computing this coefficient in the prominence region through the paper, a value representative of typical densities in prominences, while the value in the corona is adjusted taking into account the prominence-corona contrast ratio ρ_2/ρ_1 used in each calculation.

4.2. Normal mode analysis

We consider the normal mode decomposition and write the temporal dependence of the perturbation as $e^{-i\omega t}$. We Fourier analyze in the spatial directions where the medium is uniform and write the perturbations as $e^{ik_x x + ik_y y}$, with k_x and k_y the wavenumbers in the x and y-directions, respectively, and $\mathbf{k} = k_x\hat{x} + k_y\hat{y}$ the wavenumber parallel to the surface.

Then, we combine Eqs. (22) and arrive at a system of two coupled equations for v_z, the z-component of the velocity (normal to the surface) and b_x, the x-component of the perturbation of the magnetic field (along the equilibrium magnetic field)

$$\begin{aligned} i\omega c_{\rm A}^2(\omega^2 - k_x^2 c_{\rm s}^2)\frac{db_x}{dz} - \frac{i g k_y^2 \omega^2 c_{\rm A}^2(\omega + i\eta_{\rm A} k_x^2)}{\omega^2 + i k_x^2(\omega\eta_{\rm A} - i c_{\rm A}^2)}\,b_x = \\ \omega c_{\rm s}^2(\omega + i k_x^2\eta_{\rm A})\frac{d^2 v_z}{dz^2} - g\omega(\omega + i k_x^2\eta_{\rm A})\frac{dv_z}{dz} \\ + \left[\omega(\omega^2 - k^2 c_{\rm s}^2)(\omega + i k_x^2\eta_{\rm A}) - k_x^2 c_{\rm A}^2(\omega^2 - k_x^2 c_{\rm s}^2)\right]\,v_z, \end{aligned} \tag{27}$$

$$\begin{aligned} \frac{dv_z}{dz} &= \eta_{\rm A}\left\{-k_x^2 c_{\rm A}^2(\omega^2 - k_x^2 c_{\rm s}^2) + \omega(\omega^2 - k^2 c_{\rm s}^2)(\omega \right. \\ &+ \left. i k_x^2\eta_{\rm A})\right\} / \left\{(\omega^2 - k_x^2 c_{\rm s}^2)(\omega^2 - k_x^2 c_{\rm A}^2 \right. \\ &+ \left. i\omega\eta_{\rm A} k_x^2)\right\}\frac{d^2 b_x}{dz^2} + \left\{i(\omega + i k_x^2\eta_{\rm A})[-k^2 c_{\rm A}^2(\omega^2 \right. \\ &- \left. k_x^2 c_{\rm s}^2) + \omega(\omega^2 - k^2 c_{\rm s}^2)(\omega + k^2\eta_{\rm A})]\right\} / \left\{(\omega^2 \right. \\ &- \left. k_x^2 c_{\rm s}^2)(\omega^2 - k_x^2 c_{\rm A}^2 + i\omega\eta_{\rm A} k_x^2)\right\}\,b_x. \end{aligned} \tag{28}$$

We can further operate these equations to obtain a single differential equation,

$$C_4\frac{d^4 b_x}{dz^4} + C_3\frac{d^3 b_x}{dz^3} + C_2\frac{d^2 b_x}{dz^2} + C_1\frac{db_x}{dz} + C_0\,b_x = 0, \tag{29}$$

with the following definitions for the coefficients,

$$\begin{aligned} C_4 &= \omega c_{\rm s}^2\eta_{\rm A}, \\ C_3 &= -g\omega\eta_{\rm A}, \\ C_2 &= i c_{\rm A}^2(\omega^2 - k_x^2 c_{\rm s}^2) + \omega\left[\omega^2\eta_{\rm A} + c_{\rm s}^2(i\omega - 2k^2\eta_{\rm A})\right], \\ C_1 &= -ig\omega(\omega + i k^2\eta_{\rm A}), \\ C_0 &= i\left[-k^2 c_{\rm A}^2(\omega^2 - k_x^2 c_{\rm s}^2)\right. \\ &\quad \left. + \omega(\omega^2 - k^2 c_{\rm s}^2)(\omega + i k^2\eta_{\rm A})\right]. \end{aligned} \tag{30}$$

This ordinary differential equation is valid in each zone, with the equilibrium quantities $c_{\rm A}^2$, $c_{\rm s}^2$ and $\eta_{\rm A}$ with subscripts 1 or 2 when applied to the two regions above and below the contact surface at $z=0$, respectively.

Finally, we need the boundary conditions to match the solutions at the boundary $z=0$. In ideal MHD the continuity of the normal component of the velocity perturbation and the continuity of the total pressure are enough, plus the contribution of gravity from the momentum balance at the boundary. However, in this particular problem additional constraints are necessary. We derive these conditions by integrating Eqs. 21 across the surface $z=0$ and doing the limit of infinitesimal integration volume. We obtain only four independent jump relations, namely

$$\begin{aligned} \left[\rho_0 c_{\rm s}^2 v_z\right] &= 0, \\ \left[\rho_0(i\omega c_{\rm A}^2 b_x - i k_x c_{\rm s}^2 v_x - i k_y c_{\rm s}^2 v_y + c_{\rm s}^2 v_z' - g v_z)\right] &= 0, \\ \left[i k_x\eta_{\rm A} b_z - v_z + \eta_{\rm A} b_x'\right] &= 0, \\ \left[\eta_{\rm A} b_x\right] &= 0, \end{aligned} \tag{31}$$

where the prime represents a derivative on the z-direction and $[X] = X_2(0^+) - X_1(0^-)$ stands for the jump of the quantity X across $z=0$. Expressing the components of the perturbed velocity in terms of b_x and v_z we obtain the set of jump relations required for our system (since v_z requires the integral of b_x). The first relation is just the typical boundary condition for the velocity perturbation (since $\rho_0 c_{\rm s}^2 = \gamma p_0$ is equal in both sides due to the equilibrium pressure balance), and the second is related to the momentum balance (the first term is related to the magnetic pressure, the next three to the gas pressure and the last one to the gravity force), but the remaining two conditions come from the new terms

from the induction equation, which for $\eta_{\rm A}=0$ do not give any additional information. In terms of v_x and b_z our final set of boundary conditions is

$$\begin{aligned}
[v_z] &= 0,\\
\left[i\omega\rho_0\frac{c_{\rm A}^2(\omega^2-k_x^2c_{\rm s}^2)+\omega c_{\rm s}^2(\omega+ik^2\eta_{\rm A})}{\omega^2-k_x^2c_{\rm s}^2}\,b_x\right.&\\
\left.+\,\rho_0 g v_z+\frac{\omega^2c_{\rm s}^2\eta_{\rm A}b_x'}{\omega^2-k_x^2c_{\rm s}^2}\right] &= 0,\\
\left[\frac{\eta_{\rm A}b_x'-v_z}{\omega+ik_x^2\eta_{\rm A}}\right] &= 0,\\
[\eta_{\rm A}b_x] &= 0,
\end{aligned}\tag{32}$$

We use the standard definition for the linear growth rate of the instability, $\mathrm{Im}(\omega)$. Hence, $\mathrm{Im}(\omega)>0$ is related to unstable modes, while $\mathrm{Im}(\omega)<0$ marks a damping in the wave. We also define the density contrast ρ_2/ρ_1 and $\beta=c_{\rm s2}^2/c_{\rm A2}^2=c_{\rm s1}^2/c_{\rm A1}^2=\gamma\mu p_2/B_0^2$ as a measure of the magnetic field strength compared with the pressure terms.

4.3. Fully ionized plasma

Before dealing with the full problem, we check the known limit of ideal MHD. This is achieved by considering a fully ionized plasma and letting $\eta_{\rm A}\to 0$. In this case, the equations are highly simplified, and Eq. (29) just becomes

$$\frac{d^2b_x}{dz^2}-\frac{g\omega^2}{\Omega}\frac{db_x}{dz}+\frac{\omega^2-(k_x^2+k_y^2)\Omega}{\Omega}\,b_x=0,\tag{33}$$

with $\Omega=\omega^2(c_{\rm A}^2+c_{\rm s}^2)-k_x^2c_{\rm A}^2c_{\rm s}^2$. We also obtain the relation

$$\frac{dv_z}{dz}=i\omega\frac{g\omega^2b_x-\omega\Omega b_x'}{(\omega^2-k_x^2c_{\rm A}^2)(\omega^2-k_x^2c_{\rm s}^2)}\tag{34}$$

This differential equation describes the propagation of ideal MHD modes. For example, inserting a solution $b_x=Ae^{ik_zz}$ we recover the well-known dispersion relation for the MHD fast and slow modes present when gravity is not taken into account. Moreover, by imposing $\eta_{\rm A}\to 0$ the boundary conditions in Eqs. 32 reduce to the continuity of the normal component of the velocity perturbation and the continuity of the total pressure (plus a gravity term), with the two extra conditions either identically vanishing or reducing to those, and thus recovering ideal MHD boundary conditions.

We can study the linear phase regime of the compressible MHD RTI by solving Eq. (33). The solutions of its indicial (characteristic) equation obtained after setting $b_x=A_{\rm ind}e^{mz}$ (with $A_{\rm ind}$ an arbitrary constant) are

$$m_\pm=\frac{g\omega^2}{2\Omega}\pm\left(k_x^2+k_y^2-\frac{\omega^4}{\Omega}+\frac{g^2\omega^4}{4\Omega^2}\right)^{1/2}.\tag{35}$$

We need to choose the solution in each region that guarantees the perturbation to vanish far from the discontinuity. Hence, the solution is

$$b_x(z)=\begin{cases}A_1\,e^{m_1+z}, & z<0,\\ A_2\,e^{m_2-z}, & z>0,\end{cases}\tag{36}$$

with A_1 and A_2 being constants. Applying the remaining boundary conditions in Eq. (32) we obtain the dispersion relation for the system

$$\begin{aligned}
&\rho_1\left\{g+\frac{\omega^2-k_x^2c_{\rm A1}^2}{m_1}-\frac{g\omega^2(\omega^2-k_x^2c_{\rm A1}^2)}{m_1g\omega^2-m_1^2\Omega_1}\right\}=\\
&\rho_2\left\{g+\frac{\omega^2-k_x^2c_{\rm A2}^2}{m_2}-\frac{g\omega^2(\omega^2-k_x^2c_{\rm A2}^2)}{m_2g\omega^2-m_2^2\Omega_2}\right\},
\end{aligned}\tag{37}$$

There are a couple of interesting limiting cases to this expression. If we set $g=0$ we recover the solution for surface MHD waves in an interface (see, e.g., Wentzel 1979; Roberts 1981) with no instabilities, namely

$$\rho_1\frac{\omega^2-k_x^2c_{\rm A1}^2}{m_1}=\rho_2\frac{\omega^2-k_x^2c_{\rm A2}^2}{m_2},\tag{38}$$

with $m_i^2=k_x^2+k_y^2+\omega^4/\Omega_i$. Another interesting limit is the incompressible case, obtained if we set $c_{\rm si1}\to\infty$ and $c_{\rm si2}\to\infty$. The dispersion relation is then

$$\rho_1\frac{gm_1+\omega^2-k_x^2c_{\rm A1}^2}{m_1}=\rho_2\frac{gm_2+\omega^2-k_x^2c_{\rm A2}^2}{m_2},\tag{39}$$

with $m_1=k$ and $m_2=-k$ from Eq. (35) in this limit, so we can obtain an explicit equation for the frequencies of the modes,

$$\omega^2=-gk\frac{\rho_2-\rho_1}{\rho_1+\rho_2}+\frac{(\rho_1c_{\rm A1}^2+\rho_2c_{\rm A2}^2)k_x^2}{(\rho_1+\rho_2)},\tag{40}$$

which is equivalent to the classical RTI relation in Eq. (1).

After checking the limiting cases, we proceed to solve directly Eq. (37). The linear growth rate is plotted in Fig. 2, compared with the predicted rate from the classical formula in Eq. (1) for the incompressible limit. The main conclusions from these results are:

1. The threshold is not modified by compressibility. This can be easily demonstrated by noticing that in ideal MHD the frequency of the modes is either real or pure imaginary (Goedbloed & Poedts 2004; Goedbloed et al. 2010), so the transition from a stable to an unstable situation is necessarily at the points in which $\omega=0$ is satisfied. Inserting this condition in Eq. (37) we immediately recover

$$g=\frac{k_x^2(\rho_1c_{\rm A1}^2+\rho_2c_{\rm A2}^2)}{(\rho_2-\rho_1)k},\ \text{ or }\ \overline{c}_{\rm A}=c_{\rm crit}/\cos\theta,\tag{41}$$

   which matches with the stability criteria from Eq. (1) and Eq. (16). A magnetic field increase has a stabilizing effect, while increasing the angle between the equilibrium field and the wavevector has the opposite effect, as it happens in the incompressible limit.
2. The incompressible approximation becomes more valid as θ approaches $\pi/2$. This is caused by the fact the incompressible limit is recovered when $c_{\rm s}^2\to\infty$, which implies $\Omega\to\infty$, so terms containing the gravity in Eq. (35) and Eq. (37) are negligible. We can see in the definition of m and the dispersion relation that increasing the longitudinal wavenumber has a similar effect, and hence, the incompressible limit is a better approximation as k is increased.
3. The linear growth rate for the compressible case is always below the incompressible limit prediction. As β is lowered the linear growth rate is decreased substantially.

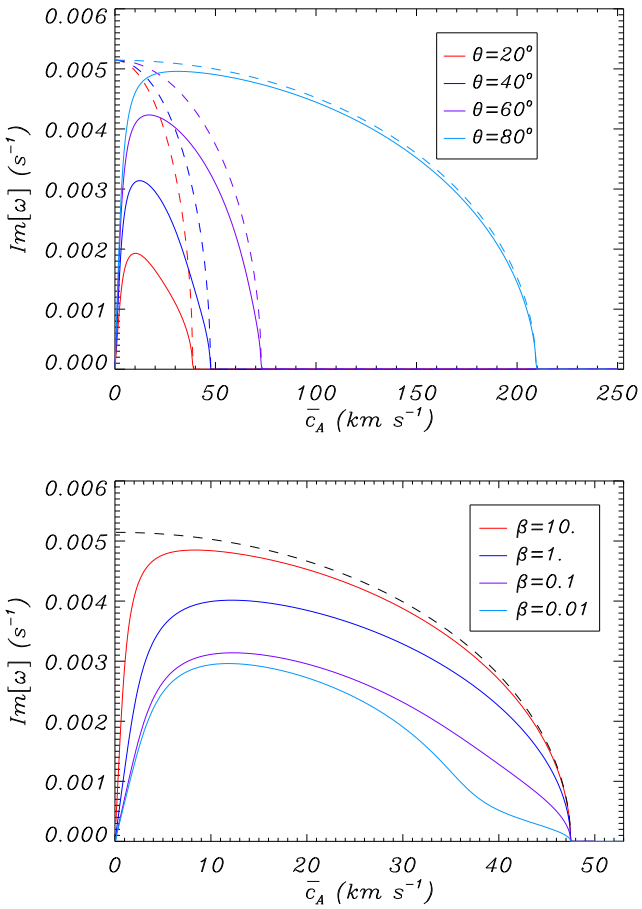

Fig. 2. Linear growth rate of the RTI for a fully ionized plasma (ideal MHD) as a function of the Alfvén speed $\overline{c}_{\rm A}$. In the upper panel curves for different values of the propagation angle θ are shown for a fixed value of $\beta = 0.1$, while in the lower panel curves for different β are plotted for a fixed value of $\theta = 40^{\rm o}$. In all the panels the values $\rho_2/\rho_1 = 100$, $g = 270$ m s^{-2} and $k = 10^{-7}$ m^{-1} have been used. The dashed curves correspond to the incompressible MHD limit in Eq. (1).

The curves in Fig. 2 tend to zero when the magnetic field is very low. This is caused by the choice of sound speed: since β is fixed in these curves, $\overline{c}_{\rm A} \to 0$ also implies that $c_{\rm s} \to 0$. If the sound speed is prevented from tending to zero as $B_0 \to 0$ (implying that β is no longer held constant and tends to zero too) the drop dissapears. There is also a real part of the frequency only when the configuration is stable in this ideal MHD regime, but we focus on the imaginary part and the instability. Leaky modes may also be considered (i.e. modes that propagate in the direction across the surface), but these modes do not appear for the range of parameters selected in these plots.

4.4. Partially Ionized Plasma

Now we turn to the general problem with the ambipolar diffusion coefficient different from zero. Eq. (29) is a fourth-order ordinary differential equation with constant coefficients, whose solutions are a combination of exponentials $e^{m_k z}$, with m_k one of the four solutions to the indicial equation

$$C_4 m^4 + C_3 m^3 + C_2 m^2 + C_1 m + C_0 = 0. \tag{42}$$

Two of these solutions are close to those in Eq. (35), while the other two are typically larger and depend strongly on the exact value of $\eta_{\rm A}$. Eq. (42) must be solved in each of the two regions, and then only the two solutions that imply evanescence away from the discontinuity are kept. The general expression of the four roots of this fourth order algebraic equation is massive, so we choose to solve it numerically. Our general solution is then

$$b_x(z) = \begin{cases} A_1\, e^{m_1^{(1)} z} + A_2\, e^{m_2^{(1)} z}, & z < 0, \\ A_4\, e^{m_3^{(2)} z} + A_3\, e^{m_4^{(2)} z}, & z > 0. \end{cases} \tag{43}$$

with the A coefficients being arbitrary constants and the subscript of m denoting the ordering of the real part among the set of m_k and the superscript the region where it applies.

The boundary conditions must be applied to obtain a dispersion relation, taking into account that v_z must be obtained by integrating Eq. (28) after inserting the solution for b_x in Eq. (43). Using the same notation that in Díaz et al. (2012), the four boundary conditions are written in matricial form as

$$\left[\sum_{j=1,4} B_{ij} b_x^{(3-j)} \right] = 0, \tag{44}$$

where the index $i \in [1,4]$ stands for the each boundary condition in Eqs. (32) and $b_x^{(j)}$ is the j-th z-derivative of b_x ($j = 0$ being the function itself without derivatives and $j = -1$ the first integral of the function). The coefficients in this matrix are given in the Appendix. Inserting the solutions from Eq. (43) in Eq. (44) we obtain a system of equations for the A-coefficients,

$$\sum_{j=1,4} (-1)^{h_k} A_k B_{ij}^{(h_k)} \left(m_k^{(h_k)} \right)^{3-j} = 0, \tag{45}$$

where the m-coefficients are defined in Equation (42), with the requirement that the exponentials are bounded at $z \to \pm\infty$. In this expression $h_k = 1$ for $k = 1, 2$ and $h_k = 2$ for $k = 3, 4$ The dispersion relation of the system is obtained by requiring the determinant of such system to vanish, namely

$$|C_{ik}| = 0, \tag{46}$$

with the C-matrix defined as

$$C_{ik} = (-1)^{h_k} \sum_{j=1,4} B_{ij}^{(h_k)} \left(m_k^{(h_k)} \right)^{3-j}. \tag{47}$$

The imaginary part of the solutions to Eq. (46) are plotted in Fig. 3, with the growth rates predicted by the incompressible and compressible RTI overplotted. The following points must be emphasized:

1. A similar plot to Fig. 3 with higher values of θ would draw the collisional plasma results closer to the incompressible MHD limit and modify the critical speed. Thus, the incompressible limit is a much better approximation as θ is increased, as happened in the collisionless plasma.

2. The instability threshold is no longer the one predicted by Eq. (1), namely $\overline{c}_{\rm A} = c_{\rm crit}/\cos\theta = 47.4$ km s^{-1} for the parameters used in the plot. In fact, *the configuration is unstable for all the values of ξ_n and magnetic field.* Considering the presence of neutrals only with the linear ambipolar term is enough to render the configuration with a heavier partially ionized fluid unstable, no matter how strong the magnetic field is.
3. For parameters which are classically unstable ($\overline{c}_{\rm A} < c_{\rm crit}/\cos\theta$) the linear growth rate is much reduced with respect to Eq. (1) because of the compressibility. Increasing the ambipolar coefficient raises slightly the growth rate, but the effect of the ambipolar term is small compared with compressibility in this range.
4. For parameters which are classically stable ($\overline{c}_{\rm A} > c_{\rm crit}/\cos\theta$) the ambipolar diffusion still drives the instability, but the linear growth rate in this regime is an order of magnitude smaller than in the classically unstable range.
5. Close to the stability threshold ($\overline{c}_{\rm A} \approx c_{\rm crit}/\cos\theta$) the differences induced by the ambipolar diffusion term are relatively higher.
6. In any case, in all the parameter space the growth rate is significantly lower than the one of an uncoupled neutral gas subject to the hydrodynamic RTI (Eq. 1 with $B_0 = 0$, ρ_{n1} and ρ_{n2}), which would be $Im[\omega] = 0.0053$ s^{-1} for the parameters in the plot. The collisional coupling between neutrals and charged particles prevents the neutrals from fully developing their instability, even for values of ξ_{n2} close to 1.
7. As the ionization fraction is raised (and thus ξ_{n2} and ξ_{n1} are lowered) the curve resembles more the MHD limit. In fact, there is a bifurcation very close to the critical value which can not be clearly seen in the scale of these plots and its value tends to $c_{\rm crit}/\cos\theta$ as the neutral fraction tends to zero.

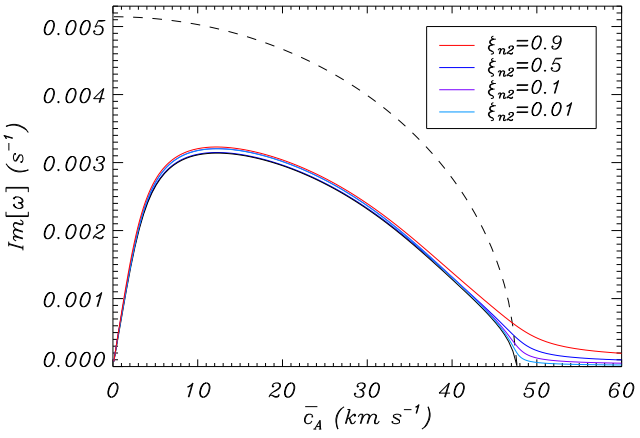

Fig. 3. Linear growth rate of the RTI for a partiallyl ionized plasma (taking into account ambipolar diffusion) as a function of the Alfvén speed $\overline{c}_{\rm A}$. The dashed line corresponds to the incompressible limit given in Eq. (1) and the black solid line to the compressible MHD results from Sect. 4.3. The values $\rho_2/\rho_1 = 100$, $\beta = 0.1$, $\theta = 40$, $k = 10^{-7}$ m^{-1}, $c_{\rm crit} = 33$ km s^{-1} and $\xi_{n1} = 10^{-4}$ have been used.

Note that with the inclusion of the ambipolar term the frequencies of the modes are no longer restricted to be either pure real or pure imaginary as in the ideal MHD limit (collisionless plasma). The solutions plotted in Fig. 3 have a real conterpart $Re[\omega]$ not shown in the plot, which is close to the compressible MHD results when $\overline{c}_{\rm A} > c_{\rm crit}/\cos\theta$ and much smaller than $Im[\omega]$ when $\overline{c}_{\rm A} < c_{\rm crit}/\cos\theta$. We can check that there is no critical value of $\overline{c}_{\rm A}$ for which the system becomes stable: if we require $\omega \to 0$, the only real solution is $c_{\rm crit} = 0$, confirming the numerical results in Fig. 3 and the absence of a stable region in the parameter space.

Another important parameter is the perturbation wavenumber k. So far we have fixed a value of $k = 10^{-7}$ m^{-1}, following the typical wavenumbers from the fast transversal MHD modes of a prominence thread used in previous studies in prominence seismology and RTI instability in threads (Díaz et al. 2002; Terradas et al. 2012; Díaz et al. 2012), but we can explore further the effects of the initial perturbation. One important consequence is obtained after scaling the problem: it can be shown that in the ideal MHD limit the curves can be rescaled using the variables $\omega/(ck)$ and $\overline{c}_{\rm A}/c$ (with c a characteristic speed, such as Alfvén speed in the prominence, for example), but if the ambipolar diffusion is included, this scaling involves the adimensional quantity $\eta_{\rm A}k/c$. Hence, increasing the wavenumber perturbation has the direct effect of increasing the relevance of the ambipolar term. This is expected, since it is known that the ambipolar diffusion grows as the typical lenght scale is reduced. On the other hand, we can also plot the linear growth rate as a function of the perturbation wavenumber (Fig. 4). We see the same main effects: there is no stable regime, the compressibility lowers the growth rate for $\overline{c}_{\rm A} < c_{\rm crit}/\cos\theta$ and the ambipolar diffusion slightly raises it as ξ_{n2} is increased. It is also interesting to study this dependence near the incompressible limit with values of θ close to 90^o (Fig. 5); since compressibility is no longer dominant, the inclusion of the ambipolar term raises the growth rate over the classical RTI (as reported in Shadmehri et al. (2013) for the same assumptions that Díaz et al. (2012) in the context of local bubble of the solar system).

Finally, we can plot the growth rate vs. the ambipolar diffusivity (Fig. 6). As mentioned above, the rate is slightly modified if the configuration is unstable in the ideal MHD limit ($\overline{c}_{\rm A} < c_{\rm crit}/\cos\theta$, upper panel), unless a very unrealistical high value of the ambipolar diffusivity is assumed. For configurations that are close to the critical value (middle panel) the dependence on the ambipolar diffusivity is more important. In the stable range ($\overline{c}_{\rm A} > c_{\rm crit}/\cos\theta$, lower panel) the linear growth rate is never zero (so strictly speaking the configuration is unstable), but the linear growth rate is at least about an order of magnitude lower than the values in classically unstable regime for typical values of $\eta_{\rm A}$, so in practice the instability would take an excessively long time to develop.

5. Full induction equation

We have dealt in the previous section with the effect of the induction term and the ambipolar diffusion term alone in the generalized induction equation for partially ionized plasmas (Eq. 15). Considering only these terms has allowed us to solve analytically the linearized equations, but the

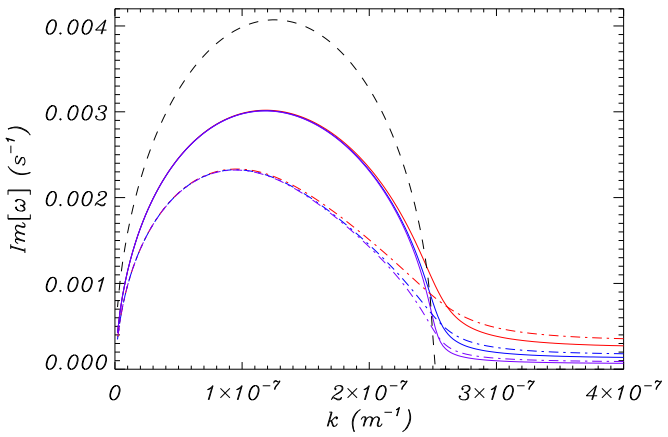

Fig. 4. Linear growth rate of the RTI for a partiallyl ionized plasma as a function of perturbation wavenumber k. The dashed line corresponds to the incompressible limit given in Eq. (1). The values $\rho_2/\rho_1 = 100$, $\theta = 40$, $\overline{c}_{\rm A} = 30$ and $\xi_{n1} = 10^{-6}$ have been used. Solid lines are calculated with $\beta = 0.1$ and dot-dashed lines with $\beta = 0.5$, while red lines have a value for the neutral fraction $\xi_{n2} = 0.9$, blue lines $\xi_{n2} = 0.5$ and purple lines $\xi_{n2} = 0.1$.

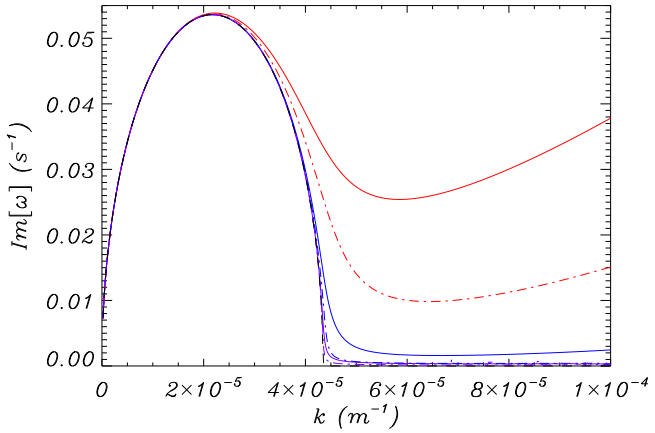

Fig. 5. Same plot as in Fig. 4 for the values of $\theta = 89$ and $\overline{c}_{\rm A} = 100$ (near the incompressible limit). Here the values of the beta are $\beta = 0.01$ in the solid lines and $\beta = 0.1$ in the dashed lines.

effect of the other supposedly smaller terms must be taken into account. In this case, obtaining analytical solutions can be much more demanding, even in the linearized problem.

5.1. Linearized equations

In order to solve this problem, first we need to eliminate the partial pressures and the density of each species in the induction equation. This can be done using the definition of the partial pressure $p_\alpha = n_\alpha k_{\rm B} T_\alpha$, and invoking that the temperature of each species is the same ($T_i = T_e = T_n$). Hence,

$$p = p_i + p_e + p_n = 2p_e + p_n = p_e(2 + \xi_n/\xi_i), \qquad (48)$$

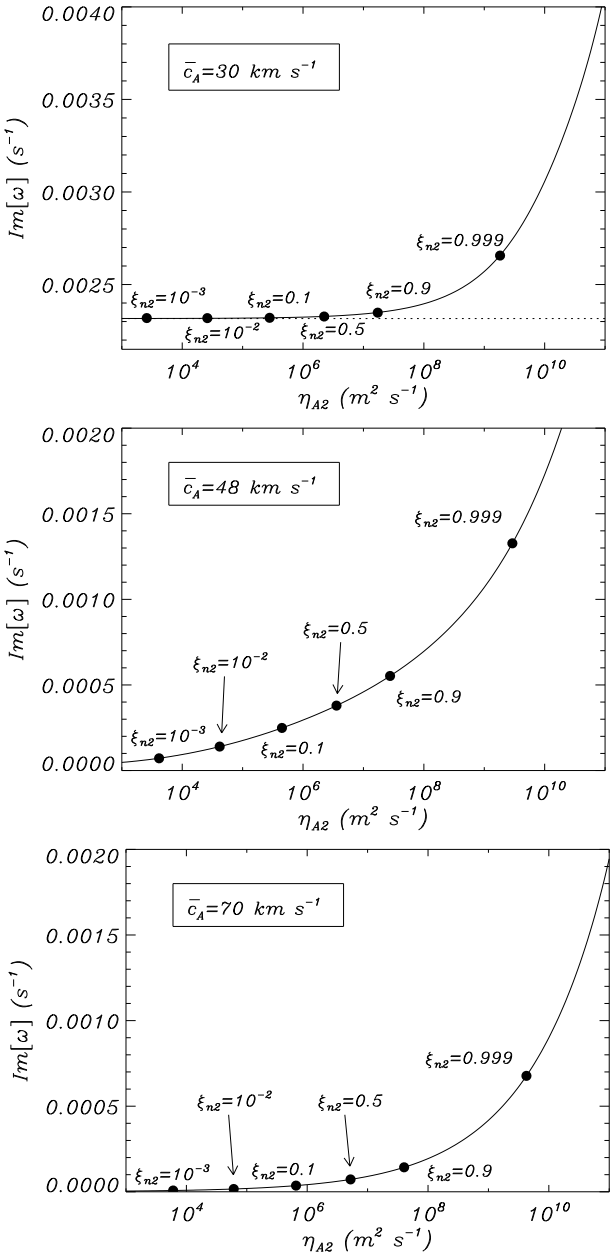

Fig. 6. Linear growth rate of the RTI for a partiallyl ionized plasma as a function of the ambipolar diffusion coefficient $\eta_{\rm A2}$, with some values of the neutral fraction ξ_{n2} for which the values of $\eta_{\rm A2}$ are obtained also included in the plot as large points. The values $\rho_2/\rho_1 = 100$, $\beta = 0.1$, $k = 10^{-7}$ m^{-1}, $\theta = 40^o$ and $\xi_{n1} = 10^{-6}$ have been used (so $c_{\rm crit} = 47$ km s^{-1}). The upper panel corresponds to a classically unstable configuration, the middle panel to a marginally stable configuration and the lower panel to a classically stable configuration. The dotted line in the upper panel corresponds to the MHD limit (in the middle and lower panel the classical limit is zero).

and we obtain

$$p_e = \frac{1-\xi_n}{2-\xi_n}\,p; \quad p_n = \frac{\xi_n}{1-\xi_n}\,p; \quad \rho_e = \frac{m_e}{m_i}(1-\xi_n)\rho, \qquad (49)$$

so we can operate Eq. (9) to obtain an expression for the pressure gradients in the battery term,

$$\mathbf{G} = \frac{\xi_n(1-\xi_n)}{2-\xi_n}\nabla p, \tag{50}$$

$$\frac{\varepsilon\mathbf{G}-\nabla p_e}{en_e} = \frac{m_e}{e\rho_e}\frac{1-\xi_n}{2-\xi_n}(\varepsilon\xi_n-1)\nabla p = \frac{m_i}{e}\frac{\varepsilon\xi_n-1}{2-\xi_n}\frac{\nabla p}{\rho}. \tag{51}$$

Here it is explicit that for a fully ionized plasma ($\xi_n = 0$) the $\mathbf{G}$ combination vanishes and the only contribution to the battery term in that case is the well-known form of the electron pressure gradient.

Next, we linearize the fluid equations. The only difference with the system in Eqs. (21) is the linear version of the induction equation. Regarding the generalized battery term, the curl of Eq. (51) is

$$\begin{aligned}\nabla\times\frac{\varepsilon\mathbf{G}-\nabla p_e}{en_e} &= \frac{m_i}{e}\frac{\varepsilon\xi_n-1}{2-\xi_n}\nabla\times\frac{\nabla p}{\rho}\\ &= \frac{m_i}{e}\frac{\varepsilon\xi_n-1}{2-\xi_n}\nabla\frac{1}{\rho}\times\nabla p,\end{aligned} \tag{52}$$

and since the equilibrium state has both the density and pressure constant in each zone, this term is at least of second order in perturbed quantities and can be neglected in the linear analysis. Taking this into account the linear version of the induction equation is

$$\begin{aligned}\frac{\partial\mathbf{b}}{\partial t} = \nabla\times\Big(&\mathbf{v}\times\mathbf{B}_0 + \eta\nabla^2\mathbf{b} + \eta_{\rm H}\left\{(\nabla\times\mathbf{b})\times\mathbf{B}_0\right\}\\ &+ \eta_{\rm A}\left\{(\nabla\times\mathbf{b})\times\mathbf{B}_0\right\}\times\mathbf{B}_0 + \eta_G/(\rho_0 c_{\rm s}^2)\nabla p\times\mathbf{B}_0\\ &- \chi_{\rm g1}/\rho_0\left[\rho_0\mathbf{g}\times\mathbf{b} + \rho\,\mathbf{g}\times\mathbf{B}_0\right]\Big),\end{aligned} \tag{53}$$

where $\eta_{\rm A}$ is given in Eq. (26) and the other diffusion coefficients can be expressed also in terms of the ionization fraction and the equilibrium parameters,

$$\begin{aligned}\eta &= \frac{m_i m_e}{\mu e^2}\frac{1}{\rho_0(1-\xi_n)}\left[\nu_{en}(\xi_n)+\nu_{ei}(\xi_n)\right] -\\ &\quad\frac{m_e^2}{\mu e^2}\frac{(\nu_{en}(\xi_n))^2}{\alpha_n(\xi_n)},\\ \eta_{\rm H} &= \frac{m_i}{\mu e}\frac{1}{\rho_0(1-\xi_n)}\left[1-\frac{\sqrt{2}}{5}\frac{m_e}{m_i}\xi_n\right],\\ \chi_{\rm G} &= \rho_0 c_{\rm s}^2\frac{\xi_n^2}{\alpha_n}\frac{1-\xi_n}{2-\xi_n},\\ \chi_{\rm g1} &= \rho_0\frac{\xi_n^2}{\alpha_n}\frac{m_e}{m_i}(1-\xi_n).\end{aligned} \tag{54}$$

Eliminating the perturbed pressure and density we obtain the following set of partial differential equations for the components of the perturbed velocity and magnetic field,

$$\begin{aligned}\frac{\partial^2\mathbf{v}}{\partial t^2} &= \frac{1}{\mu\rho_0}(\nabla\times\mathbf{b})\times\mathbf{B}_0 - (\nabla\cdot\mathbf{v})\,\mathbf{g} + c_{\rm s}^2\nabla(\nabla\cdot\mathbf{v}),\\ \frac{\partial^2\mathbf{b}}{\partial t^2} &= \nabla\times\left(\frac{\partial\mathbf{v}}{\partial t}\times\mathbf{B}_0\right) + \eta\nabla^2\frac{\partial\mathbf{b}}{\partial t}\\ &\quad - \eta_{\rm H}\nabla\times\left\{\left(\nabla\times\frac{\partial\mathbf{b}}{\partial t}\right)\times\mathbf{B}_0\right\}\\ &\quad + \eta_{\rm A}\left\{\left(\nabla\times\frac{\partial\mathbf{b}}{\partial t}\right)\times\mathbf{B}_0\right\}\times\mathbf{B}_0\\ &\quad + \chi_{\rm G}\nabla\times\left\{\nabla(\nabla\cdot\mathbf{v})\times\mathbf{B}_0\right\}\\ &\quad + \chi_{\rm g1}\left[\left\{\nabla(\nabla\cdot\mathbf{v})\right\}\times(\mathbf{g}\times\mathbf{B}_0) - (\mathbf{g}\cdot\nabla)\frac{\partial\mathbf{b}}{\partial t}\right],\end{aligned} \tag{55}$$

The complexity of these equations is evident, and even third order derivatives are present in the term coming from $\mathbf{G}\times\mathbf{B}$. Finding direct analytical solutions is still possible in our problem if we notice that all the coefficients are constant in each region of our model, so we obtain a third order linear system of six equations, whose solutions are written in terms of linear combinations of exponential functions.

5.2. Normal mode analysis

We again consider the normal mode decomposition with the temporal dependence as $e^{-i\omega t}$ and the dependence on the directions where the equilibrium state is uniform as $e^{ik_x x+ik_y y}$. Now we can eliminate v_x, v_y and b_z to obtain the three differential equations, which are given in the Appendix. We obtain four solutions that go to zero as $z\to\infty$ and other four that go to zero as $z\to-\infty$, so the general solution in each zone would be a linear combination of the four linearly independent solutions that satisfy the boundary condition as $|z|\to\infty$ in each region.

Next we need to derive the boundary conditions appropiate to this problem, and following the procedure used in the case of ambipolar diffusion alone, we go directly to Eqs. 55 and integrate them across the boundary, obtaining only five relations between the variables

$$\begin{aligned}\left[\rho_0 c_{\rm s}^2 v_z\right] &= 0,\\ \Big[\rho_0\left\{i\omega c_{\rm A}^2 b_x c_{\rm s} - ik_x c_{\rm s}^2 v_x - ik_y c_{\rm s}^2 v_y\right.&\\ \left.- g v_z + c_{\rm s}^2 v_z'\right\}\Big] &= 0,\\ \Big[\eta_{\rm A}(ik_x\omega b_z + \omega b_x') - \eta\omega b_x' - ik_x\omega b_y\eta_{\rm H}&\\ + \chi_{\rm G}c_{\rm s}^2(-ik_y^2 v_z + k_x v_x' + k_y v_y' + iv_z'')&\\ - g\chi_{\rm g1}(\omega b_x + k_x v_x + k_y v_y + iv_z') - \omega v_z\Big] &= 0,\\ \left[ik_x\left(\omega b_x\eta_{\rm H} + k_y c_{\rm s}^3\chi_{\rm G}v_z\right) - \omega\eta b_y' - g\omega b_y\chi_{\rm g1}\right] &= 0,\\ \Big[k_x\omega\eta_{\rm A}b_x + i\omega\eta b_z' - igk_x c_{\rm s}\chi_{\rm g1}v_z&\\ + k_x c_{\rm s}^3\chi_{\rm G}\left(k_x v_x + k_y v_y + iv_z'\right)\Big] &= 0.\end{aligned} \tag{56}$$

However, these relations are not enough for our problem, which has four arbitrary constants in each side of the boundary. The divergence-free condition $\nabla\cdot\mathbf{b} = 0$ and the expressions for the perturbed pressure and density in Eqs. 21 only give us linear combinations of the conditions in Eq. 56. To obtain the additional relations we need to use the equation for the diffusion velocity between ions and neutrals (which introduces the higher-order derivatives in the linearized equations). The linear version of Eq. (11) is

$$\mathbf{w} = \eta_{\rm A}\left[\nabla\times\frac{\partial\mathbf{b}}{\partial t}\right]\times\mathbf{B}_0 + \chi_{\rm G1}\nabla(\nabla\cdot\mathbf{v})$$

$$+\ \eta_{\rm H1}\nabla\times\frac{\partial \mathbf{b}}{\partial t}-\chi_{\rm g2}(\nabla\cdot\mathbf{v})\,\mathbf{g}=0, \quad (57)$$

with the coefficients defined as

$$\eta_{\rm H1}=\frac{\xi_n\nu_{ne}\rho_0}{n_e e\mu\alpha_n},\ \ \chi_{\rm G1}=\frac{\rho_0}{\xi_n}\chi_{\rm G},\ \ \chi_{\rm g2}=\frac{1}{\xi_n}\chi_{\rm g1}. \quad (58)$$

Using this equation, we obtain the remaining three jump relations for our system, namely

$$\begin{aligned}\Big[\alpha_n\left(\omega b_y\eta_{\rm H1}-ik_x c_{\rm s}\chi_{\rm G1}v_z\right)\Big] &= 0,\\ \Big[\alpha_n\left(-i\omega b_x\eta_{\rm H1}-ik_y c_{\rm s}\chi_{\rm G1}v_z\right)\Big] &= 0,\\ \Big[\alpha_n\left(i\omega\eta_{\rm A}b_x-gc_{\rm s}\chi_{\rm g2}v_z-ik_x c_{\rm s}\chi_{\rm G1}v_x\right.&\\ \left.-ik_y c_{\rm s}\chi_{\rm G1}v_y+c_{\rm s}\chi_{\rm G1}v_z'\right)\Big] &= 0. \end{aligned} \quad (59)$$

which provides us with the remaining conditions to solve the linear problem. Notice that we recover easily the case with ambipolar diffusion alone, since the first two equations vanish in this case and the last one becomes equivalent to the last jump condition in Eq. (31).

5.3. Numerical solutions

The solution of the problem must be computed in the following form: first of all, the differential equations in Eq. A.3 for b_x, b_y and v_z must be solved in each zone by obtaining the set of solutions for λ from Eq. A.6 (and the relation between the constants of each variable), and then discarding the solutions that not vanish as $|z|\to 0$. This leaves us with solutions with four arbitrary constants in each zone. Finally, the jump conditions in Eqs. (56) and (59) must be satisfied, which can only be achieved is the determinant of the system of this eight equation vanishes. This provides us with a dispersion relation for computing the frequencies of our system, and thus, studying the stability of the system by checking if their imaginary parts are either positive (unstable modes) or negative (stable modes).

The procedure described in the previous paragraph does not give simple analytical solutions, so we use it to find numerical solutions to the system. It is important to remark that these solutions are not obtained from partial differential equations, but from an algebraic system of equations. There is a huge range of parameters that can be explored, but here we concentrate on the situations of physical interest for the RTI instability, namely, when all the diffusive terms are much lower than the induction term. All the η and χ coefficients in these diffusive terms depend on the ionization fraction ξ_n due to their dependence on the densities, collisions frequencies and temperatures.

First of all, we study the numerical values and dependence of the different collision frequencies, since we also need the collisional frequencies of electrons with other species, which are (Soler et al. 2009; Braginskii 1965)

$$\nu_{en}=\frac{\rho_n}{m_{\rm n}}\sqrt{\frac{16k_{\rm B}T}{\pi m_{\rm n}}}\,\sigma_{\rm en},\quad \nu_{ei}=\frac{n_e}{T^{3/2}}\Lambda h_{\rm ei}, \quad (60)$$

where $\sigma_{\rm en}\approx 10^{-19}$ m^2, $h_{\rm ei}\approx 3.7\times10^{-6}$ s^{-1} m^{-3} K$^{3/2}$ and Λ is the Coulomb logarithm. We plot these frequencies in terms of the ionization fraction in Fig. 7 for values of the parameters typical in prominences, namely $\rho_0=10^{-10}$ kg m^{-3}, $p_0=0.135$ Pa and $B_0=10$ G, so $c_{\rm s}=15$ km s^{-1} and $c_{\rm A}=89$ km s^{-1}. For fully ionized plasmas the neutral collision frequencies vanish, as expected, but as the ionization fraction is increased it becomes comparable and even larger than the collision frequency between ions and electrons. Note that the assumption in Soler et al. (2012b); Díaz et al. (2012) of neglecting the electron collisions might not be appropiate for these values of the plasma parameters (specially for low values of ξ_n).

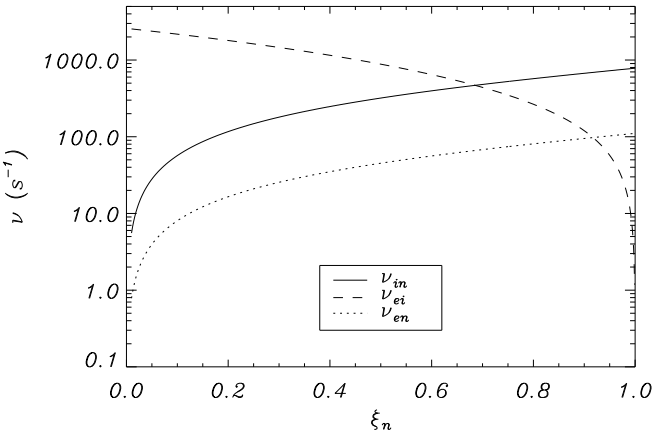

Fig. 7. Collisional frequencies as a function of the ionization fraction for the values of the density, pressure and magnetic field given in the text.

Next we study the different terms in the linearized induction equation (Eq. 55). The values of each term are represented in Fig 8 for typical values of $k_x=k_y=10^{-7}$ m^{-1}, $g=270$ m s^{-1} and $Im[\omega]\approx 0.007$ s^{-1}, normalized to the magnitude of the ideal MHD induction term $\nabla\times(\mathbf{v}\times\mathbf{B}_0)$. The dominant term under these plasma conditions is the ambipolar term, which was studied independently in the previous section. Then the Hall and perpendicular battery terms are typically about one order of magnitude smaller than the ambipolar, and finally the gravity and ohmic diffusion terms are much lower. Note that for a fully ionized plasma $\xi_n\to 0$ the ambipolar, battery and gravity terms tend to zero, but the hall and ohmic terms are still present. In addition, the battery term neglected in the linearization (Eq. 51) would also be present for a fully ionized plasma.

Next we study the solutions of the indicial equation (Eq. A.6). There are four solutions that are very close to the ones in Eq. (42), and four new ones that are related to the other diffusion coefficients and are about four order of magnitude larger (and thus describe only diffusive effects very near the boundary and are negligible far from it). However, these diffusive solutions are troublesome from the computational point of view, since they introduce large coefficients in the boundary conditions that must be computed with great accuracy.

Finally we can obtain the frequency of the modes of the system. We concentrate on the relevant modes to the stability analysis. The imaginary part of the frequency is plotted near the instability threshold in Fig. 9 for a typical set of parameters in prominence thread oscillations. The differences between the ambipolar result and the full equations

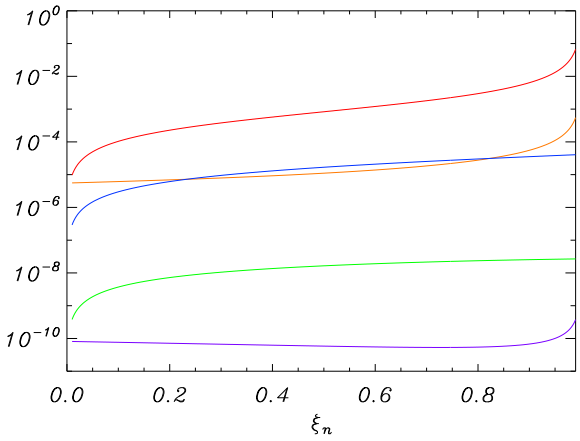

Fig. 8. Numerical values of the terms in the induction equation in Eq. (55) relative to the ideal MHD term, with the values stated in the text. The red line corresponds to the ambipolar term, the blue line to the Hall term, the orange line to the perpendicular battery term ($\mathbf{G} \times \mathbf{B}$), the green line to the gravity terms and the purple line to the Ohmic term.

are small, but one interesting difference is that in the MHD stable regime (which corresponds to $k_x > 1.3 \cdot 10^{-7}$ m-1 for these parameters) the inclusion of the rest of the term in the induction equation raises the linear growth rate slightly, while in the MHD unstable regime ($k_x < 1.3 \cdot 10^{-7}$ m-1) it lowers it slightly, but the corrections are small compared with the computed values for the ambipolar case. Hence, as expected from Fig. 8 the rest of the terms offer just slightly corrections to the results for the ambipolar case described in Sect. 4, at least for the physical and plasma parameters in prominences.

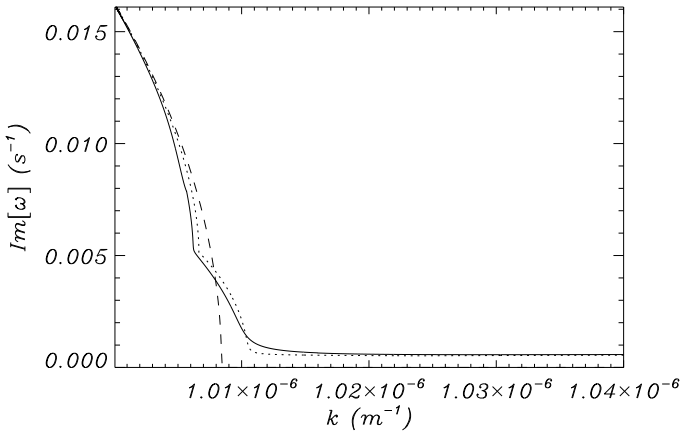

Fig. 9. Linear growth rate of the RTI as a function of the wavenumber. The values chosen for the plot are $\rho_2 = 10^{-10}$ kg m^{-3}, $\rho_2/\rho_1 = 100$, $\theta = 85^o$ m^{-1}, $B_0 = 10$ G, c_{s2}=15 km s^{-1}, $\xi_2 = 0.5$ and $\xi_1 = 0.1$. The dashed line is the incompressible MHD limit from Eq. (1), the dotted line corresponds to the PI 1-fluid model with only the ambipolar term (section 4) and the solid line to the PI 1-fluid model with all the terms in the induction equation.

It is very interesting to notice that the PI effects do not modify qualitatively the linear growth rate in the region of classical stability. This is in contradiction with the result in Díaz et al. (2012), who reported in their Section 5 that the linear growth rate was lowered by an order of magnitude. However, in that calculation a very low value of the equilibrium density was chosen to compute ν_{in}, so it would correspond to the case in which the ambipolar coefficient is chosen to be larger than the value obtained in this work. We can see in Fig. 9 that the effects of PI do not lower that drastically the linear growth rate for this set of parameters. We obtain from Fig. 9 a typical RTI timescale of about 100 s, similar to the lifetime of prominence threads (Labrosse et al. 2010; Mackay et al. 2010; Lin 2011).

6. Discussion and conclusions

We have studied the effects of considering a partially ionized plasma in the MHD Rayleigh-Taylor instability in a contact surface where a heavier plasma sits on top of a lighter one. We have simplified considerably the problem by assuming that the equilibrium variables are uniform in each region, which is only valid if the vertical scales of the perturbations are much smaller than the gravitational scale height. In fact, in the initial stages of the instability the solution is confined to the boundary, so this approximation is useful. However, in later stages the gravity stratification may become important, but then the differential equations may become too hard to be solved analytically, and the problem is better posed in terms of numerical studies, which would also allow to characterize the non-linear phases of the instability.

Including PI effects in the MHD equations can be done in several ways. In Díaz et al. (2012) a two-fluid model was considered, with the collisions between ions and neutrals only deemed important. Here we have taken a different approach by using all the collision frequencies between the species, but combining the fluid equations for each species into 1-fluid equations (following Braginskii 1965, for example). These PI effects appear then in the form of a generalized Ohm's law (Eq. 12) and induction equation (Eq. 13), with the corresponding terms in the energy equation (which are second order effects in the linear analysis). We follow the standard procedure of deriving a relation for the diffusion velocity between ions and neutrals from the equation of motion for electrons (with the electron inertial terms neglected). However, in contrast with previous deductions we have kept all the terms, obtaining the well known expressions for the ohmic, ambipolar, Hall and battery diffusion terms, but also the $\mathbf{G} \times \mathbf{B}$ (similar to the Hall term with diamagnetic currents) and the gravity term. This gravity effect has been normally overlooked because it comes from neglecting the electron gravity force in front of the ion gravity force on the combined momentum equation for ions and electrons, but we have proved that this term survives as the equation for the diffusion velocity is obtained. Under prominence thread circumstances, this term is nevertheless small, but can be still larger than the ohmic diffusion, and might also be relevant in other contexts.

It has been previously assessed that the most important term in the generalized Ohm's law is the ambipolar diffusion term (Khomenko & Collados 2012). We first study the modifications that this term implies in the linear regime. An ordinary differential equation is derived with constant

coefficients because of the uniform plasma assumption in each zone, so a solution close to the ideal-MHD is found, with another related to the ambipolar coefficient. The ordinary MHD jump relations are not enough, so following Chandrasekhar (1961) we derive our boundary relations directly from the differential equations, obtaining new conditions to add to the continuity of total pressure are perpendicular velocity. Finally the modes of the system are obtained, with the MHD-limit recovered when $\eta_{\rm A} \to 0$. The main conclusions are that the configuration is always unstable regardless of the values of the parameters, but in the region of the parameter space where there was classical stability the linear growth rate is very small, while in the classically stable region the ambipolar slightly raises the linear growth rate compared with the compressible MHD limit. These results support the conclusions in Díaz et al. (2012) and qualitatively both descriptions agree despite considering different assumptions on the fluid equations. Notice however that in the 2-fluid description Díaz et al. (2012) considered that the collision frequency of both media were simply related by ρ_2/ρ_1 and used a high value of equilibrium density, while here we have derived a relation between the ambipolar diffusion coefficients in both regions considering all the dependence of the equilibrium parameters on ξ_n in both regions.

Next we consider the full induction equation, checking first the relevance of the different terms in the linear analysis. It is found that the battery and gravity terms do not give any direct contribution in the linear regime in a uniform equilibrium medium, but their Hall counterparts still appear. The other terms are orders of magnitude smaller than the ambipolar term. The problem is solved in a similar way, with extra solutions to the indicial equation because of these dissipative terms. The numerical analysis of the solutions confirms that for typical values of prominence threads they only induce small corrections to the results of the ambipolar case.

A direct application of the results of this paper concerns solar prominence threads. It is widely assumed that chromospheric material sits on top of a less dense coronal plasma, either in a static equilibrium or dynamical configurations. The RTI has been studied numerically in such configurations (Hillier et al. 2011, 2012a), so it is interesting to test the differences that PI effects produce, specially taking into account that the material that forms the prominence is expected to be partially ionized (despite the ionization fraction has not been directly measured so far). A plot of the linear growth rate for different values of the equilibrium field is displayed in Fig. 10. The effects described in our analysis can be summarized as:

- There is no critical value, the configuration is always unstable to the RTI instability because of the presence of neutrals.
- On the region of classical stability, the PI terms give a small linear growth rate, so the time-scale of the instability is much larger than the typical lifetime of the threads.
- On the region of classical instability, the PI affects also the growth rate, but this rate is still very high (despite a stabilizing effect of the compressibility), so the RTI is very efficient and can disrupt the threads.
- For typical prominence plasma parameters, the PI effects are small, since the ambipolar term is much smaller than the MHD induction term (Fig. 8) and the perturbation is nearly incompressible (Terradas et al. 2012). However, if the term is larger than the theoretical values the effect becomes more pronounced (see the plot for a high $\eta_{\rm A}$ value in Fig. 10).
- The leading ambipolar term becomes important on small scales (for the typical prominence parameters whose scales are expected to be in the range of 100 km and below). Current observational facilities are almost at this limit (for example the Japanese HINODE mission, or Sunrise/IMaX instrument) and the new generation of telescopes (such as ATST or EST) are aimed to provide information on such scales. Thus, we are about to be able to observe the spatial range where the PI effects in prominences might be directly observed).
- Including other additional PI terms beyond the leading ambipolar term only give small numerical changes (mainly near the classical critical value) at the price of a much harder analytical and computational effort.

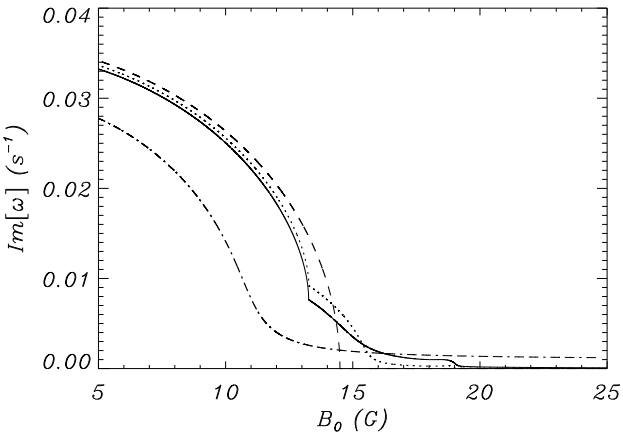

Fig. 10. Linear growth rate vs. equilibrium magnetic field for $\rho_2/\rho_1 = 100$, $g = 270$ m s^{-2}, $\theta = 87^o$, $k = 5 \cdot 10^{-6}$ m^{-1}, $\xi_{n1} = 10^{-4}$, $\rho_2 = 10^{-10}$ kg m^{-3}. The dotted line is the ambipolar case with $\xi_{n2} = 0.5$, the solid line with $\xi_{n2} = 0.05$ and the dot-dashed line to $\xi_{n2} = 0.5$, but with a value for the ambipolar diffusion coefficient 1000 times larger than the theoretical value used in the rest of the computations, while the dashed line corresponds to the incompressible MHD limit (Eq. 1).

These conclusions need to be tested in several ways. First of all, the analysis carried out in this work is only valid in the linear regime, so once the instability is triggered on, non-linearities may become important, and it is well-known from MHD simulations that once the stability is well developed secondary Kelvin-Hemholtz instabilities appear (seen as eddies in the simulations), so the linear growth rate is lowered and the drops formed reach a terminal velocity; all these processes are not present in the linear analysis. Moreover, the battery term contribution can be neglected in the linear analysis, but helps to raise currents in the nonlinear regime. More crucially, no new effects are present in the linearized energy equation.

Another neglected effect that might be important is the presence of a density stratification (mainly due to grav-

ity), despite having typical lenghscales much larger than the thread thickness. Some studies point out that these stratification effects have a stabilizing contribution on the RTI (Liberatore et al. 2009). However, considering a non-uniform plasma in each region complicates substantially the analysis (specially the differential equations, which no longer have constant coefficients), and might change the relevance of some terms (such as the battery term, which would have a linear contribution). In this case, the problem is better posed to numerical solutions, specially considering that other effects might also be important, such as the curvature of the field lines forming the dip that sustains the condensation which constitutes the thread.

Numerical simulations are underway to study the complex effects of PI in the instability and the non-linear regime Khomenko et al. (2013). The calculations in this work offer a guide to test the results, at least in the first stages of the instability.

Acknowledgements. The authors acknowledge the financial support by the Spanish Ministry of Science through project AYA2010-18029. This work contributes to the deliverables identified in FP7 European Research Council grant agreement 277829, "Magnetic connectivity through the Solar Partially Ionized Atmosphere", whose PI is E. Khomenko (Milestone 3 and contribution toward Milestones 1).

Appendix A: Coefficients on the linear system of equations

Here we present the coefficients that appear in the linearized equations for both the ambipolar diffusion section and the general case. If only ambipolar diffusion is considered in the induction equation (Sect 4), then the boundary conditions can be written in terms of b_x, as is shown in Eq. 44

$$
\begin{aligned}
B_{11} &= 0,\\
B_{12} &= \left\{i(\omega+ik_x^2\eta_{\rm A})[-k^2c_{\rm A}^2(\omega^2-k_x^2c_{\rm s}^2)\right.\\
&+ \left.\omega(\omega^2-k^2c_{\rm s}^2)(\omega+k^2\eta_{\rm A})]\right\}/\left\{(\omega^2-k_x^2c_{\rm s}^2)(\omega^2\right.\\
&- \left.k_x^2c_{\rm A}^2+i\omega\eta_{\rm A}k_x^2)\right\},\\
B_{13} &= 0,\\
B_{14} &= \eta_{\rm A}\frac{-k_x^2c_{\rm A}^2(\omega^2-k_x^2c_{\rm s}^2)+\omega(\omega^2-k^2c_{\rm s}^2)(\omega+ik_x^2\eta_{\rm A})}{(\omega^2-k_x^2c_{\rm s}^2)(\omega^2-k_x^2c_{\rm A}^2+i\omega\eta_{\rm A}k_x^2)},\\
B_{21} &= \frac{\omega^2c_{\rm s}^2\eta_{\rm A}}{\omega^2-k_x^2c_{\rm s}^2},\\
B_{22} &= g\eta_{\rm A}\frac{k_x^2c_{\rm A}^2(\omega^2-k_x^2c_{\rm s}^2)-\omega(\omega^2-k^2c_{\rm s}^2)(\omega+ik_x^2\eta_{\rm A})}{(\omega^2-k_x^2c_{\rm s}^2)(\omega^2-k_x^2c_{\rm A}^2+i\omega\eta_{\rm A}k_x^2)},\\
B_{23} &= i\omega\frac{\omega^2(c_{\rm A}^2+c_{\rm s}^2)+i\omega k^2c_{\rm s}^2\eta_{\rm A}-k_x^2c_{\rm A}^2c_{\rm s}^2}{\omega^2-k_x^2c_{\rm s}^2},\\
B_{24} &= -g(i\omega-k_x^2\eta_{\rm A})\times\\
&\quad\frac{-k^2c_{\rm A}^2(\omega^2-k_x^2c_{\rm s}^2)+\omega(\omega^2-k^2c_{\rm s}^2)(\omega+ik^2\eta_{\rm A})}{(\omega^2-k_x^2c_{\rm s}^2)(\omega^2-k_x^2c_{\rm A}^2+i\omega\eta_{\rm A}k_x^2)},\\
B_{31} &= 0,\\
B_{32} &= \frac{k_y^2\omega c_{\rm s}^2\eta_{\rm A}}{(\omega^2-k_x^2c_{\rm s}^2)(\omega^2-k_x^2c_{\rm A}^2+i\omega\eta_{\rm A}k_x^2)},\\
B_{33} &= 0,\\
B_{34} &= \frac{ik^2c_{\rm A}^2(\omega^2-k_x^2c_{\rm s}^2)+\omega(\omega^2-k^2c_{\rm s}^2)(-i\omega+k^2\eta_{\rm A})}{(\omega^2-k_x^2c_{\rm s}^2)(\omega^2-k_x^2c_{\rm A}^2+i\omega\eta_{\rm A}k_x^2)},\\
B_{41} &= 0,\\
B_{42} &= 0,\\
B_{43} &= \eta_{\rm A},\\
B_{44} &= 0,
\end{aligned}
\tag{A.1}
$$

These coefficients are then used in Eq. 47 to compute the growth rates.

Next we present the coefficients that appear in the linearized equations for the general case, when all the terms in the induction equation are considered (Sect. 5). The method is similar to the one applied in the ambipolar case, but the complexity of the problem prevents us to write the boundary conditions in terms of a single magnitude, as it was done in the ambipolar section using b_x. First of all, from the linearized equation of motion we express v_x, v_y and b_z as

Eq. 53

$$
\begin{aligned}
v_x &= \frac{k_xc_{\rm s}\left(k_yc_{\rm A}^2(k_xb_y-k_yb_x)+i\omega c_{\rm s}v_z'\right)}{\omega^3-\omega c_{\rm s}^2\left(k_x^2+k_y^2\right)},\\
v_y &= \frac{c_{\rm A}^2\left(k_x^2c_{\rm s}^2-\omega^2\right)(k_yb_x-k_xb_y)+ik_y\omega c_{\rm s}^3v_z'}{\omega^3c_{\rm s}-\omega c_{\rm s}^3\left(k_x^2+k_y^2\right)},\\
b_z &= \left[ik_x^2c_{\rm A}^2c_{\rm s}^2b_x'-i\omega^2c_{\rm A}^2b_x'+igk_y^2c_{\rm A}^2b_x+ik_xk_yc_{\rm A}^2c_{\rm s}^2b_y'\right.\\
&- igk_xk_yc_{\rm A}^2b_y+g\omega c_{\rm s}v_z'+k_x^2\omega c_{\rm s}^3v_z+k_y^2\omega c_{\rm s}^3v_z\\
&- \left.\omega c_{\rm s}^3v_z''-\omega^3c_{\rm s}v_z\right]/\left[k_xc_{\rm A}^2\left(c_{\rm s}^2\left(k_x^2+k_y^2\right)-\omega^2\right)\right],
\end{aligned}
\tag{A.2}
$$

Next, we can write each of the three components of the induction equation as

$$
\sum_{j=1}^{4}\alpha_{ij}b_x^{(j-1)}+\sum_{j=1}^{4}\beta_{ij}b_y^{(j-1)}+\sum_{j=1}^{5}\gamma_{ij}v_z^{(j-1)}=0,
\tag{A.3}
$$

where $i=1,2,3$ is the component of the induction equation and $b_x^{(j)}$ stands for the $j^{\rm th}$-derivative of b_x, for example. The coefficients in this equations are

$$
\begin{aligned}
\alpha_{11} &= c_{\rm A}^2c_{\rm s}\left[i\omega\left\{c_{\rm s}^2\left(k_x^2+k_y^2\right)\left(-k_y^2\eta_{\rm A}+\left(k_x^2+k_y^2\right)\eta+i\omega\right)\right.\right.\\
&+ k_y^2\omega^2\eta_{\rm A}+igk_y^3\eta_{\rm H}-\omega^2\left(k_x^2+k_y^2\right)\eta\Big\}\\
&+ \left.k_y^2c_{\rm A}^2\left(-\omega^2+c_{\rm s}^2\left(k_x^2-ik_y^2\omega\chi_{\rm G}\right)\right)+\omega^4\right],\\
\alpha_{12} &= -i\omega c_{\rm A}^2c_{\rm s}\left[g\chi_{\rm g1}\left(k_y^2c_{\rm A}^2+c_{\rm s}^2\left(k_x^2+k_y^2\right)-\omega^2\right)\right.\\
&+ \left.gk_y^2\eta_{\rm A}+ik_y\eta_{\rm H}\left(\omega^2-k_x^2c_{\rm s}^2\right)\right],\\
\alpha_{13} &= i\omega c_{\rm A}^2c_{\rm A}\left[c_{\rm A}^2\left(k_y^2\left(c_{\rm A}^2\chi_{\rm G}+\eta_{\rm A}\right)-\left(k_x^2+k_y^2\right)\eta\right)+\omega^2\eta\right],\\
\alpha_{14} &= 0,\\
\alpha_{21} &= k_xk_yc_{\rm A}^2c_{\rm s}\left[c_{\rm A}^2\left(\omega^2-c_{\rm s}^2\left(k_x^2-ik_y^2\omega\chi_{\rm G}\right)\right)\right.\\
&+ \left.i\omega\eta_{\rm A}\left(c_{\rm s}^2\left(k_x^2+k_y^2\right)-\omega^2\right)+gl\omega\eta_{\rm H}\right],\\
\alpha_{22} &= -k_xk_y^2\omega c_{\rm A}^2c_{\rm s}^3\eta_{\rm H},\\
\alpha_{23} &= \alpha_{24}=0,\\
\alpha_{31} &= \omega c_{\rm A}^2c_{\rm s}\left[gk_x^2\chi_{\rm g1}\left(k_y^2c_{\rm A}^2+c_{\rm s}^2\left(k_x^2+k_y^2\right)-\omega^2\right)\right.\\
&+ gk_x^2k_y^2\eta_{\rm A}+k_y\left(-gk_y\left(k_x^2+k_y^2\right)\eta\right.\\
&- \left.\left.i\left(k_x^2\eta_{\rm H}\left(c_{\rm s}^2\left(k_x^2+k_y^2\right)-\omega^2\right)+gk_y\omega\right)\right)\right],\\
\alpha_{32} &= \omega c_{\rm A}^2c_{\rm s}\left[\omega^2\left(\left(k_x^2+k_y^2\right)\eta+i\omega\right)\right.\\
&- \left.k_x^2c_{\rm s}^2\left(k_y^2\left(c_{\rm A}^2\chi_{\rm G}+\eta_{\rm A}+\eta\right)+k_x^2\eta+i\omega\right)\right],\\
\alpha_{33} &= gk_y^2\omega c_{\rm A}^2c_{\rm s}\eta,\\
\alpha_{34} &= \omega c_{\rm A}^2c_{\rm s}\eta\left(k_x^2c_{\rm s}^2-\omega^2\right),
\end{aligned}
$$

$$
\begin{aligned}
\beta_{11} &= k_x k_y c_{\rm A}^2 c_{\rm s} \left[c_{\rm A}^2 \left(\omega^2 - c_{\rm s}^2 \left(k_x^2 - i k_y^2 \omega \chi_{\rm G}\right)\right)\right. \\
&+ \left. i\omega\eta_{\rm A} \left(c_{\rm s}^2 \left(k_x^2 + k_y^2\right) - \omega^2\right) + g k_y \omega \eta_{\rm H}\right], \\
\beta_{12} &= k\omega c_{\rm A}^2 c_{\rm s} \left(\eta_{\rm H} \left(k_x^2 c_{\rm s}^2 - \omega^2\right) + i g k_y \left(c_{\rm A}^2 \chi_{\rm g1} + \eta_{\rm A}\right)\right), \\
\beta_{13} &= -i k_x k_y \omega c_{\rm A}^2 c_{\rm s}^3 \left(c_{\rm A}^2 \chi_{\rm G} + \eta_{\rm A}\right), \\
\beta_{14} &= 0, \\
\beta_{21} &= c_{\rm A}^2 c_{\rm s} \left[i\omega \left(-c_{\rm s}^2 \left(k_x^2 + k_y^2\right) \left(k_x^2 \eta_{\rm A} - \left(k_x^2 + k_y^2\right)\eta - i\omega\right)\right.\right. \\
&+ k_x^2 \left(\omega^2 \eta_{\rm A} + i g k_y \eta_{\rm H}\right) - \omega^2 \left(k_x^2 + k_y^2\right)\eta \\
&+ \left.\left. k_x^2 c_{\rm A}^2 \left(-\omega^2 + c_{\rm s}^2 \left(k_x^2 - i k_y^2 \omega \chi_{\rm G}\right)\right) + \omega^4\right], \\
\beta_{22} &= -i\omega c_{\rm A}^2 c_{\rm s} \left[g\chi_{\rm g1} \left(c_{\rm s}^2 \left(k_x^2 + k_y^2\right) - \omega^2\right) + i k_x^2 k_y c_{\rm s}^2 \eta_{\rm H}\right], \\
\beta_{23} &= -i\omega c_{\rm A}^2 c_{\rm s} \eta \left(c_{\rm s}^2 \left(k_x^2 + k_y^2\right) - \omega^2\right), \\
\beta_{24} &= 0, \\
\beta_{31} &= k_x \omega c_{\rm A}^2 c_{\rm s} \left[g k_y \chi_{\rm g1} \left(-k_x^2 c_{\rm A}^2 + c_{\rm s}^2 \left(k_x^2 + k_y^2\right) - \omega^2\right)\right. \\
&- g k_x^2 k_y \eta_{\rm A} + i \left(k_x^2 \eta_{\rm H} \left(c_{\rm s}^2 \left(k_x^2 + k_y^2\right) - \omega^2\right) + g k_y \omega\right) \\
&+ \left. g k_y \left(k_x^2 + k_y^2\right)\eta\right], \\
\beta_{32} &= k_x k_y \omega c_{\rm A}^2 c_{\rm s}^3 \left(k_x^2 \left(c_{\rm A}^2 \chi_{\rm G} + \eta_{\rm A}\right) - \left(k_x^2 + k_y^2\right)\eta - i\omega\right), \\
\beta_{33} &= -g k_x k_y \omega c_{\rm A}^2 c_{\rm s} \eta, \\
\beta_{34} &= k_x k_y \omega c_{\rm A}^2 c_{\rm s}^3 \eta,
\end{aligned}
$$

$$
\begin{aligned}
\gamma_{11} &= i k_y \omega^2 c_{\rm s}^2 \eta_{\rm H} \left(c_{\rm s}^2 \left(k_x^2 + k_y^2\right) - \omega^2\right), \\
\gamma_{12} &= \omega c_{\rm s}^2 \left[i c_{\rm A}^2 \left(\omega^2 - c_{\rm s}^2 \left(k_x^2 - i k_y^2 \omega \chi_{\rm G}\right)\right)\right. \\
&+ \left. \omega \eta_{\rm A} \left(\omega^2 - c_{\rm s}^2 \left(k_x^2 + k_y^2\right)\right) + i g k_y \omega \eta_{\rm H}\right], \\
\gamma_{13} &= \omega^2 c_{\rm s}^2 \left(-g \left(c_{\rm A}^2 \chi_{\rm g1} + \eta_{\rm A}\right) - i k_y c_{\rm s}^2 \eta_{\rm H}\right), \\
\gamma_{14} &= \omega^2 c_{\rm s}^4 \left(c_{\rm A}^2 \chi_{\rm G} + \eta_{\rm A}\right), \\
\gamma_{15} &= 0, \\
\gamma_{21} &= -i k_x \omega^2 c_{\rm s}^2 \eta_{\rm H} \left(c_{\rm s}^2 \left(k_x^2 + k_y^2\right) - \omega^2\right), \\
\gamma_{22} &= k_x \omega c_{\rm s}^2 \left(k_y c_{\rm A}^2 c_{\rm s}^2 \left(\omega \chi_{\rm G} - i\right) - i g \omega \eta_{\rm H}\right), \\
\gamma_{23} &= i k_x \omega^2 c_{\rm s}^4 \eta_{\rm H}, \\
\gamma_{24} &= \gamma_{25} = 0, \\
\gamma_{31} &= \omega c_{\rm s}^2 \left[\omega^2 - c_{\rm s}^2 \left(k_x^2 + k_y^2\right)\right) \left(-k_x^2 c_{\rm A}^2 + \omega \left(i k_x^2 \eta_{\rm A}\right.\right. \\
&- \left.\left. i \left(k_x^2 + k_y^2\right)\eta + \omega\right)\right], \\
\gamma_{32} &= -i g \omega^2 c_{\rm s}^2 \left(k_x^2 \left(c_{\rm A}^2 \chi_{\rm g1} + \eta_{\rm A}\right) - \left(k_x^2 + k_y^2\right)\eta - i\omega\right), \\
\gamma_{33} &= i\omega^2 c_{\rm s}^2 \left[\omega^2 \eta + c_{\rm s}^2 \left(k_x^2 \left(c_{\rm A}^2 \chi_{\rm G} + \eta_{\rm A}\right) - 2\left(k_x^2 + k_y^2\right)\eta\right.\right. \\
&- \left.\left. i\omega\right)\right], \\
\gamma_{34} &= -i g \omega^2 c_{\rm s}^2 \eta, \\
\gamma_{35} &= i\omega^2 c_{\rm s}^4 \eta. \qquad \text{(A.4)}
\end{aligned}
$$

The solution of the system of differential equations with constant coefficients can be obtaining by a combination of exponentials in the form

$$b_x = A_1\, e^{\lambda z},\ b_y = A_2\, e^{\lambda z},\ v_z = A_3\, e^{\lambda z}, \qquad \text{(A.5)}$$

with A_1, A_2 and A_3 arbitrary coefficients. This type of solution leads to the system of algebraic equations

$$A_1 \sum_{j=1}^{4} \alpha_{ij} \lambda^{j-1} + A_2 \sum_{j=1}^{4} \beta_{ij} \lambda^{j-1} + A_3 \sum_{j=1}^{5} \gamma_{ij} \lambda^{j-1} = 0, \qquad \text{(A.6)}$$

whose non-vanishing solutions are only obtained if the determinant of the system is zero. This gives the indicial equation, which turns out to be a $8^{\rm th}$ order algebraic equation in λ. There is no simple way of expressing the solutions of this equation in terms of the coefficients of the system, but for the range of parameters under considerations, there are always four solutions with $\mathrm{Re}[\lambda] \geq 0$ and four with $\mathrm{Re}[\lambda] \leq 0$, and can be further grouped in pairs with $\mathrm{Re}[\lambda_1] \approx -\mathrm{Re}[\lambda_2]$ and $\mathrm{Im}[\lambda_1] \approx \mathrm{Im}[\lambda_2]$, provided the diffusion coefficients are small. It is easy to check that if all the diffusion coefficients except the ambipolar one are set to zero the 8-th order equation becomes Eq. (42), so two of the solutions are $\lambda \approx m_1^{(1)}$ and $\lambda \approx m_2^{(1)}$ (and similar expression in the upper zone), provided the diffusion terms are small, while the other two have much larger real part than these two, representing exponentials that decay very fast from the boundary. Finally, for each solution of the indicial equation we find a relation between the A-coefficients in Eq. (A.5), so for each value of λ all the perturbed velocity and magnetic field components can be related to b_x, for example.

References

Arber, T. D., Haynes, M., & Leake, J. E. 2007, ApJ, 666, 541
Balescu, R. 1988, Transport processes in a plasma (Amsterdam, North Holland)
Berger, T., Testa, P., Hillier, A., et al. 2011, Nature, 472, 197
Berger, T. E., Shine, R. A., Slater, G. L., et al. 2008, ApJ, 676, L89
Berger, T. E., Slater, G., Hurlburt, N., et al. 2010, ApJ, 716, 1288
Bernstein, I. B. & Book, D. L. 1983, Physics of Fluids, 26, 453
Bittencourt, J. A. 1986, Fundamentals of plasma physics (Oxford: Pergamon Press)
Braginskii, S. I. 1965, Transport Processes in Plasma, ed. M. A. Leontovich (New York, USA: Consultants Bureau), 201–311
Breitschwerdt, D., Freyberg, M. J., & Egger, R. 2000, A&A, 361, 303
Bucciantini, N., Amato, E., Bandiera, R., Blondin, J. M., & Del Zanna, L. 2004, A&A, 423, 253
Chandrasekhar, S. 1961, Hydrodynamic and Hydromagnetic Stability (CUP, New York: Dover Publications Inc., 1932)
Chhajlani, R. K. & Vaghela, D. S. 1989, Ap&SS, 155, 257
Díaz, A. J., Oliver, R., & Ballester, J. L. 2002, ApJ, 580, 550
Díaz, A. J., Soler, R., & Ballester, J. L. 2012, ApJ, 754, 41
Drazin, P. G. & Reid, W. H. 1981, Hydrodynamic stability, Vol. 82 (Cambridge Mathematical Library), 17950
Eggleton, P. P., Dearborn, D. S. P., & Lattanzio, J. C. 2006, Science, 314, 1580
Forteza, P., Oliver, R., Ballester, J. L., & Khodachenko, M. L. 2007, A&A, 461, 731
Fryxell, B., Arnett, D., & Mueller, E. 1991, ApJ, 367, 619
Gilbert, H., Kilper, G., & Alexander, D. 2007, ApJ, 671, 978
Goedbloed, J. P. H., Keppens, R., & Poedts, S. 2010, Advanced Magnetohydrodynamics (Cambridge)
Goedbloed, J. P. H. & Poedts, S. 2004, Principles of Magnetohydrodynamics (Cambridge)
Heinzel, P., Schmieder, B., Fárník, F., et al. 2008, ApJ, 686, 1383
Hillier, A., Berger, T., Isobe, H., & Shibata, K. 2012a, ApJ, 746, 120
Hillier, A., Hillier, R., & Tripathi, D. 2012b, ApJ, 761, 106
Hillier, A., Isobe, H., Shibata, K., & Berger, T. 2011, ApJ, 736, L1
Hillier, A., Isobe, H., Shibata, K., & Berger, T. 2012c, ApJ, 756, 110
Isobe, H., Miyagoshi, T., Shibata, K., & Yokoyama, T. 2005, Nature, 434, 478
Isobe, H., Miyagoshi, T., Shibata, K., & Yokoyama, T. 2006, PASJ, 58, 423
Jun, B.-I., Norman, M. L., & Stone, J. M. 1995, ApJ, 453, 332
Khodachenko, M. L., Arber, T. D., Rucker, H. O., & Hanslmeier, A. 2004, A&A, 422, 1073
Khomenko, E. & Collados, M. 2012, ApJ, 747, 87
Khomenko, E., Díaz, A. J., Collados, M., & De Vicente, A. 2013, A&A, in preparation
Labrosse, N., Heinzel, P., Vial, J.-C., et al. 2010, Space Sci. Rev., 151, 243
Liberatore, S. & Bouquet, S. 2008, Physics of Fluids, 20, 116101
Liberatore, S., Jaouen, S., Tabakhoff, E., & Canaud, B. 2009, Physics of Plasmas, 16, 044502
Lin, Y. 2011, Space Sci. Rev., 158, 237
Livescu, D. 2004, Physics of Fluids, 16, 118

Mackay, D. H., Karpen, J. T., Ballester, J. L., Schmieder, B., & Aulanier, G. 2010, Space Sci. Rev., 151, 333
Matsumoto, J. & Masada, Y. 2013, ApJ, 772, L1
Mitchner, M. & Kruger, C. H. 1973, Partially Ionized Gases (John Wiley and Sons, New York)
Parker, E. N. 1979, Ap&SS, 62, 135
Patsourakos, S. & Vial, J.-C. 2002, Sol. Phys., 208, 253
Priest, E. R. 1982, Solar Magnetohydrodynamics (D. Reidel Publishing Company)
Ribeyre, X., Tikhonchuk, V. T., & Bouquet, S. 2004, Physics of Fluids, 16, 4661
Roberts, B. 1981, Sol. Phys., 69, 27
Ryutova, M., Berger, T., Frank, Z., Tarbell, T., & Title, A. 2010, Sol. Phys., 267, 75
Shadmehri, M., Yaghoobi, A., & Khajavi, M. 2013, Ap&SS
Shivamoggi, B. K. 1982, Physics of Fluids, 25, 911
Shivamoggi, B. K. 2008, ArXiv e-prints
Soler, R., Andries, J., & Goossens, M. 2012a, A&A, 537, A84
Soler, R., Diaz, A. J., Ballester, J. L., & Goossens, M. 2012b, ApJ, in press (arXiv:1202.4274)
Soler, R., Oliver, R., & Ballester, J. L. 2009, ApJ, 699, 1553
Stone, J. M. & Gardiner, T. 2007, ApJ, 671, 1726
Terradas, J., Oliver, R., & Ballester, J. L. 2012, A&A, 541, A102
Vandervoort, P. O. 1961, AJ, 66, 56
Vranjes, J. & Krstic, P. S. 2013, ArXiv e-prints
Wang, Y.-M. & Nepveu, M. 1983, A&A, 118, 267
Wentzel, D. G. 1979, ApJ, 227, 319
Zaqarashvili, T. V., Khodachenko, M. L., & Rucker, H. O. 2011a, A&A, 534, A93
Zaqarashvili, T. V., Khodachenko, M. L., & Rucker, H. O. 2011b, A&A, 529, A82